CANADIAN JOURNAL OF RESEARCH

VOLUME 18 JULY, 1940 NUMBER 7

CONTENTS

NATIONAL RESEARCH COUNCIL
OTTAWA, CANADA

Publications and Subscriptions

The Canadian Journal of Research is issued monthly in four sections, as follows:

A. Physical Sciences
B. Chemical Sciences
C. Botanical Sciences
D. Zoological Sciences

For the present, Sections A and B are issued under a single cover, as also are Sections C and D, with separate pagination of the four sections, to permit separate binding, if desired.

Subscription rates, postage paid to any part of the world (effective 1 April, 1939), are as follows:

	Annual	*Single Copy*
A and B	$ 2.50	$ 0.50
C and D	2.50	0.50
Four sections, complete	4.00	—

The Canadian Journal of Research is published by the National Research Council of Canada under authority of the Chairman of the Committee of the Privy Council on Scientific and Industrial Research. All correspondence should be addressed:

National Research Council, Ottawa, Canada.

Notice to Contributors

Fifty reprints of each paper are supplied free. Additional reprints, if required, will be supplied according to a prescribed schedule of charges.

Canadian Journal of Research

Issued by THE NATIONAL RESEARCH COUNCIL OF CANADA

VOL. 18, SEC. A. JULY, 1940 NUMBER 7

RADIO FREQUENCY MEASUREMENTS OF GROUND CONDUCTIVITY IN CANADA[1]

BY K. A. MACKINNON[2]

Abstract

Ground conductivities, as determined by field strength measurements of broadcasting stations using T. L. Eckersley's approximation to Sommerfeld's propagation formula, are given for many areas in Canada. A correlation is shown to exist between the ground conductivities thus found and the geological character of the area under study. The practical utility of these measurements in the selection of sites for transmitters, and in the estimation of field strength contours therefrom, is indicated.

Introduction

It has been shown by Sommerfeld (5, 6) that the attenuation of radio waves over a plane earth is a function not only of their frequency but also of the electrical conductivity and dielectric constant of the soil over which they pass.

The difficulty encountered in making numerical computations from his formulae has led to the development of a great variety of simplified approximations. Of these, one might mention those of T. L. Eckersley (2), Norton (4), Burrows (1), Fitch and Duttera (3). For broadcast frequencies (550 to 1500 kc.) over ground of average conductivity to a distance of one hundred miles or so there is not much to choose among them. Indeed in practice it is found that the varying ground characteristics within this distance usually have a more disturbing effect than the differences indicated among the various methods of approximation.

Of the four methods, Norton's and that of Burrows are valid over a wide range of frequencies and ground constants, whereas the remaining two are at least satisfactory for broadcast frequencies (550 to 1500 kc.) over ground of average conductivity. In using these latter methods of restricted validity, one can neglect entirely the ground dielectric constant. In this paper the method of T. L. Eckersley is used for all determinations.

Fig. 1 is a graph of the approximation curves of T. L. Eckersley drawn to show field strength in millivolts per metre against distance in miles, and

[1] *Manuscript received March 13, 1940.*

Contribution from the Engineering Division, Canadian Broadcasting Corporation, Montreal, Que.

An interim report on this subject was presented before a joint meeting of the American Section of the International Scientific Radio Union (U.R.S.I.) and the Institute of Radio Engineers, held at Washington, April 30, 1938. This document may be found in the Proceedings of the General Assembly of the U.R.S.I., Sept., 1938, Volume V, Fascicule 1, Memoires Scientifiques.

[2] *Transmission and Development Engineer, Canadian Broadcasting Corporation.*

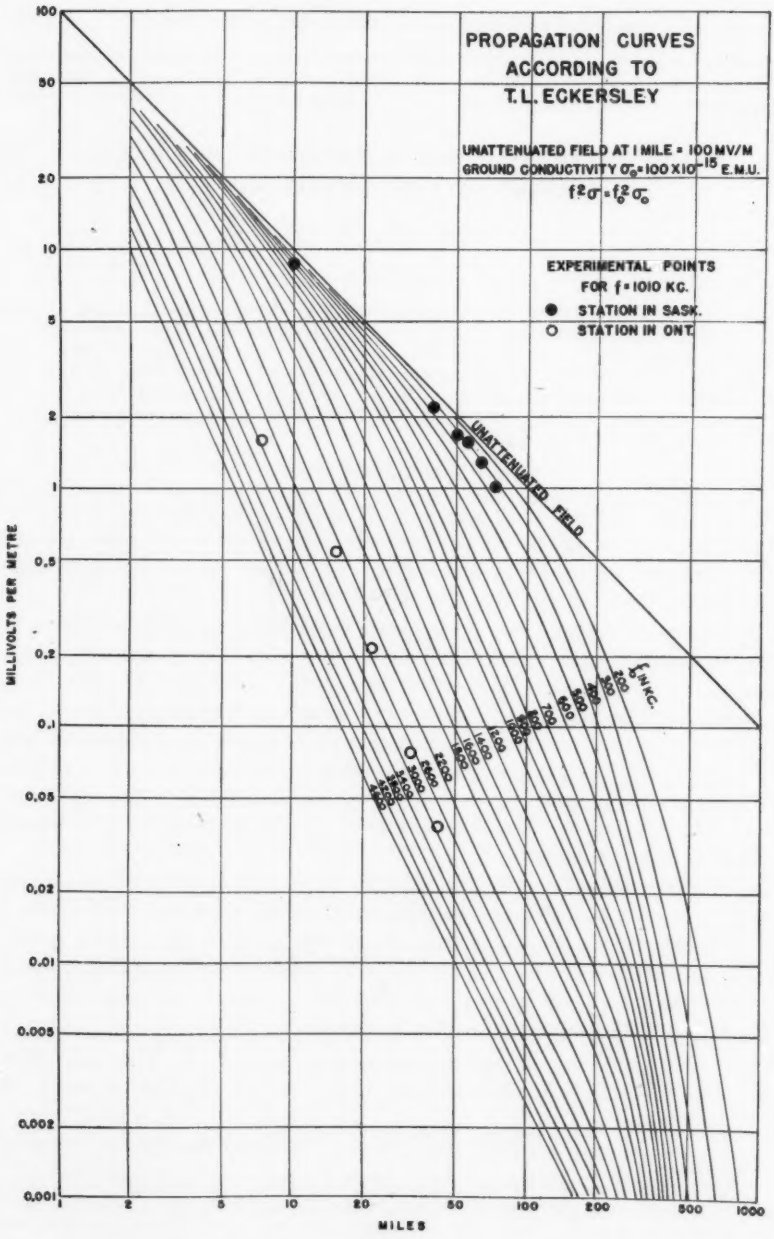
PROPAGATION CURVES
ACCORDING TO
T. L. ECKERSLEY
UNATTENUATED FIELD AT 1 MILE = 100 MV/M
GROUND CONDUCTIVITY $\sigma_0 = 100 \times 10^{-15}$ E.M.U.
$f^2\sigma = f_0^2\sigma_0$
EXPERIMENTAL POINTS
FOR f = 1010 KC.
STATION IN SASK.
STATION IN ONT.
UNATTENUATED FIELD
f_0 IN KC.
MILLIVOLTS PER METRE
MILES
100
50
20
10
5
2
1
0.5
0.2
0.1
0.05
0.02
0.01
0.005
0.002
0.001
1
2
5
10
20
50
100
200
500
1000

FIG. 1.

frequency in kilocycles per second. The unattenuated field strength at one mile from the transmitting antenna has been assumed to be 100 mv. per metre, and the ground to have a conductivity of 100×10^{-15} e.m.u.

A correction for the effect of the curvature of the earth is embodied in these curves. This effect however is not of much concern within a distance of about one hundred miles in the broadcast band of frequencies.

To determine the ground conductivity of an area over which a series of field strength measurements from a transmitter has been taken, it is first necessary to ascertain by actual measurement, or by calculation from the known physical dimensions of the radiating system, the unattenuated field strength at one mile. Here, actual measurement is to be preferred because the calculation requires certain assumptions, especially in respect to the "ohmic" losses in the ground system. A further advantage in the direct measurement lies in the fact that, providing this work is carried out with the same field strength measuring instrument as that used in the remote series of measurements, the absolute accuracy of the instrument does not enter into the conductivity determinations. In other words the plotted points become merely "attenuation" curves in which only ratios of field measurements appear. Thus in Fig. 1 by dividing the ordinates by 100 the millivolts per metre unit is changed into a simple reduction factor.

The curves indicate the propagation of waves of given frequencies (f_0) over ground of a constant conductivity (σ_0) equal to 100×10^{-15} e.m.u. For other conductivities (σ) and frequencies (f) use is made of Eckersley's approximate relation $f^2\sigma = f_0^2\sigma_0$.

To illustrate the use of the curves, points are marked on Fig. 1 representing actual field measurements of two stations both using the same frequency of 1010 kc., but located in different parts of Canada. Before plotting these measurements it was necessary of course to correct them in order to have them in terms of the same antenna efficiency of 100 mv. per metre at one mile. The Saskatchewan points are seen to trace a curve corresponding to a frequency of about 350 kc. Thus the ground conductivity over this given direction from the station is $\sigma = (f_0/f)^2 \cdot \sigma_0 = 840 \times 10^{-15}$ e.m.u. On the other hand the Ontario station points lie near the curve 2600 kc. so that σ in this direction is about 15×10^{-15} e.m.u.

The tremendous influence of ground conductivity on the attenuation of radio waves is clearly seen here, for these measurements show that at 40 miles distance one signal is some fifty times greater than the other. In other words the Ontario station using 1010 kc. needs 2500 times the power of the Saskatchewan station using the same frequency and a similar antenna in order that the same field strength be attained by each station at 40 miles in the direction given. This illustration indicates the vital importance national broadcasting authorities should attach to the collection of ground conductivity data.

Before concluding the discussion of the use of the curves, it is well to point out that the absolute value of the ground conductivity thus determined is by no means high. This is largely a result of the fact that the ground charac-

teristics are themselves usually quite variable over the miles of radial distance from a transmitter required to make a conductivity determination. Thus the plotted points may appear more or less scattered about some mean frequency value. The resulting single figure for ground conductivity therefore represents a sort of "effective" or "average" value of this property along the radial in question. Nevertheless this is the kind of figure desired, for, if the curves are valid for such an average value, the use of the figure thus determined should yield reasonably good estimates of the attenuation of different frequencies along the radial in question. To obtain such estimates of course is the ultimate aim of the broadcast engineer. In this connection it should be remembered that signal strength alone does not determine the technical excellence of reception of a broadcast program. Such of course depends rather on the signal-to-noise ratio existing at the receiving point. "Noise" here means those disturbing effects due to natural atmospherics, interfering signals from other stations or interference from man-made electrical machines. As it is not generally possible to estimate the strength of the noise signals at any given point, it is seen that there is no practical necessity for high accuracy in the field strength estimates. Experience has shown that the field strength contour representing 0.5 mv. per metre is a rough indication of the extent of the good service area of a broadcasting station. This figure is essentially a compromise since in electrically "quiet" rural areas such a signal strength is stronger than necessary, whereas in "noisy" urban centres the 0.5 mv. per metre level is much too weak.

Realizing that the ability to estimate the service areas of proposed broadcast transmitters was essential to the engineering planning of a national broadcast system, the original national radio body in Canada, The Canadian Radio Broadcasting Commission, soon after its inception in 1933 began to carry out field strength surveys of existing transmitters. The measurements were analysed in the manner above described to give figures for ground conductivities of Canadian soil. Prior to this time, it may be pointed out, no such information appeared to be available.

This work has been continued by the Canadian Broadcasting Corporation and now there are figures available for most of the parts of Canada which may be reached by automobile.

Figs. 2 and 3 show the latest available data in this regard. The point from which a group of arrows radiate is the site of an existing transmitter or the temporary location of a test transmitter. The arrows indicate the general direction of a radial along which field strength measurements were made. The figure at an arrow head when multiplied by 10^{-15} represents the average ground conductivity in electromagnetic units along that particular length of arrow.

One will contrast the very low conductivities in the Maritimes with the very high values in the Prairies. The great difference this means in the extent of the service area of transmitters otherwise identical has already been discussed. To avoid as much as possible this serious disability in the Mari-

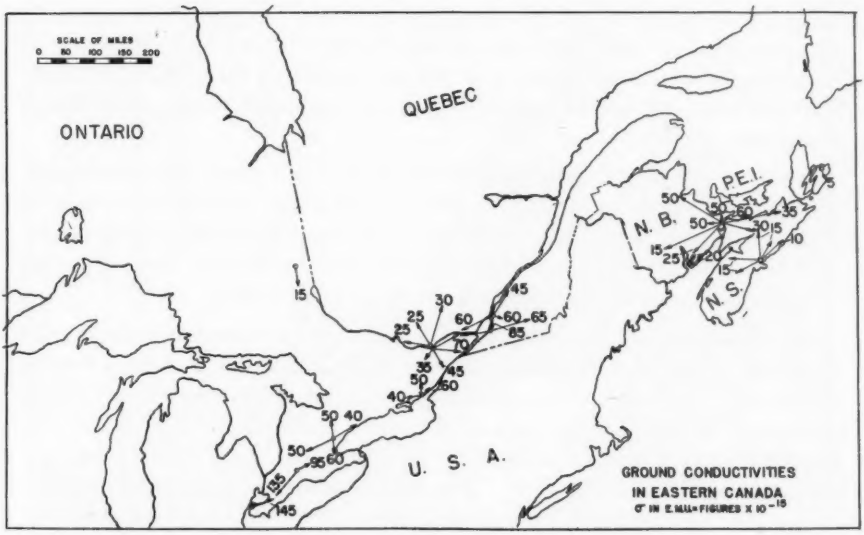
SCALE OF MILES
0 50 100 150 200
ONTARIO
QUEBEC
P.E.I.
N. B.
N. S.
U. S. A.
GROUND CONDUCTIVITIES
IN EASTERN CANADA
σ IN E.M.U.=FIGURES X 10⁻¹⁵

FIG. 2.

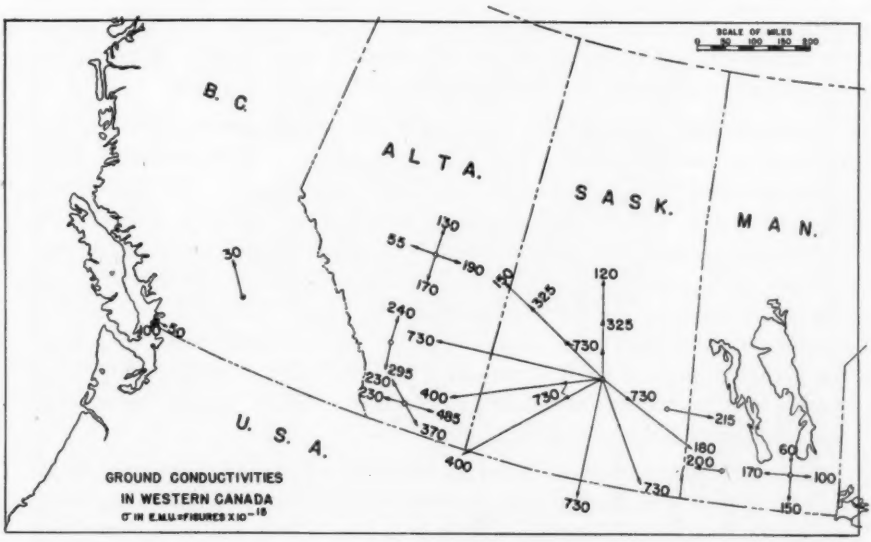
SCALE OF MILES
0 50 100 150 200
B. C.
ALTA.
SASK.
MAN.
U. S. A.
GROUND CONDUCTIVITIES
IN WESTERN CANADA
σ IN E.M.U.=FIGURES X 10⁻¹⁵

FIG. 3.

times, the regional transmitter CBA was located near Sackville. From this site the greatest advantage of the practically perfect transmission of sea water ($\sigma = 10{,}000 \times 10^{-15}$) is being taken to reach much of the populated coastal regions of these provinces. In the Prairies the very high conductivity, plus the relatively low frequency of 540 kc., permitted the CBK transmitter site to be centrally located and yet to give a strong signal in numerous distant towns and cities.

It was often the case, especially in the earlier years when the field strength measurements were sparse, that it was very desirable to have some idea of the value of the ground conductivity in a region which had never been surveyed. This led to an attempt to correlate the existing conductivity measurements with the geology of Canada, which is known in great detail.

Some connection is naturally to be expected and a comparison of the conductivity map of Figs. 2 and 3 with the geology map of Fig. 4 shows a certain correlation. For example, the three geological areas in lower southern Ontario correspond to the London area conductivity averaging 140×10^{-15}, the Hamilton area averaging around 80×10^{-15}, and the Toronto-Kingston-Ottawa area at about 50×10^{-15}. The dark areas in the Maritimes correspond to the very low conductivity values of 15×10^{-15}. The high conductivity Prairies area, which tapers off in conductivity as one comes eastward past Winnipeg, is suggested by the geology map.

Early estimates of conductivity of unsurveyed regions, based on this apparent correlation with geology, have later been confirmed by actual measurements. This correlation is still used to advantage in many day-to-day problems requiring the estimation of field strength contours.

The practical utility of these conductivity determinations is well illustrated in Fig. 5 which shows the 0.5 mv. per metre contour of CBA, Sackville, N.B., the selection of the site of which has already been discussed. The figure shows three contours. One of these (dot-dash line) was estimated in 1937 with the help of the geology map plus a few field strength measurements made near Halifax, N.S. and St. John, N.B. The second contour (dotted line) was that determined by the use of a 200 watt test transmitter with a 65 ft. mast erected at the Sackville site in 1937. The third contour (solid line) shows the actual contour of CBA as measured in 1939. The first two contours, of course, were estimated for the 50 kw. power and 455 ft. vertical mast which it was known CBA would actually use.

It is seen that the effect of the sea coast was overestimated in the area toward Chatham, N.B., and that no allowance was made for the very low conductivity range of hills between Westchester and Sackville. It is well to mention that this site is a most difficult one from which to make estimates because of the haphazard mixture of sea water and low conductivity ground.

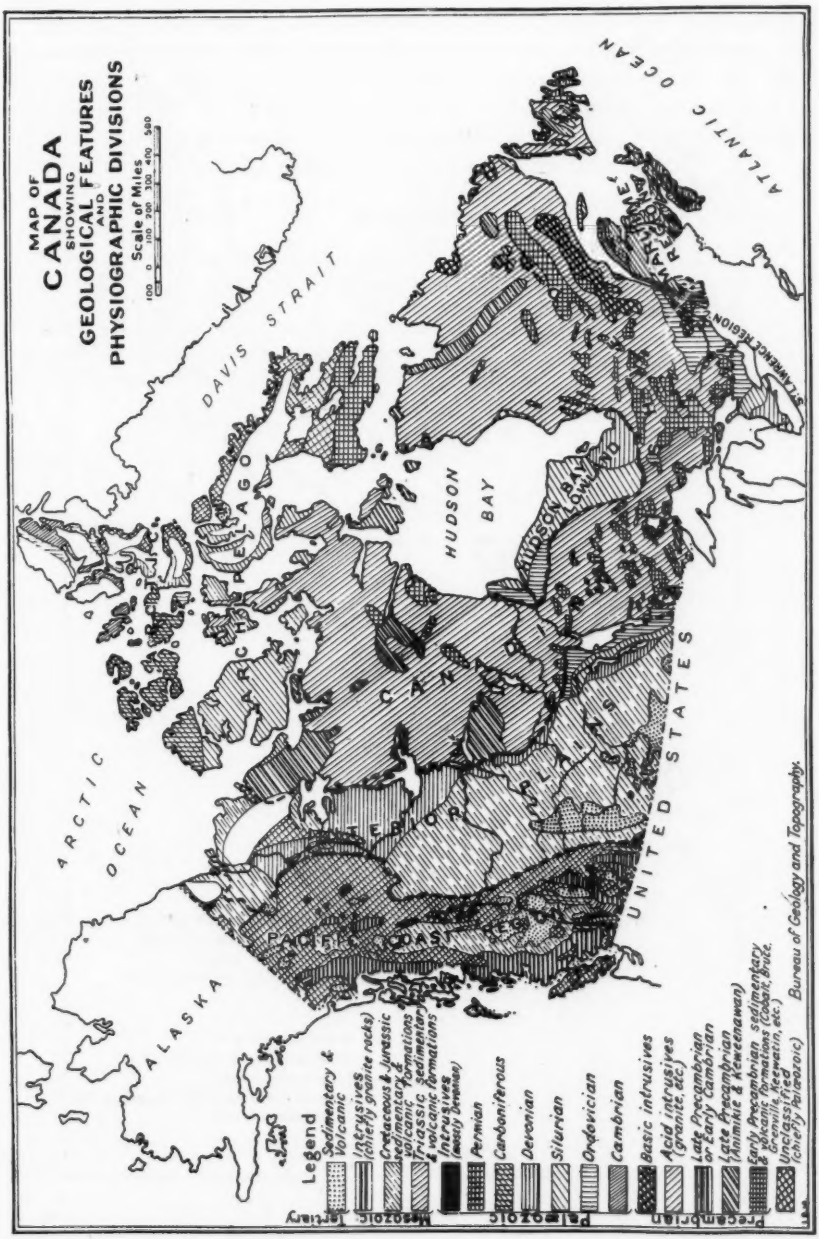
MAP OF
CANADA
SHOWING
GEOLOGICAL FEATURES
AND
PHYSIOGRAPHIC DIVISIONS
Scale of Miles
100 0 100 200 300 400 500
ARCTIC OCEAN
DAVIS STRAIT
BAFFIN ISLAND
HUDSON BAY
HUDSON BAY LOWLAND
LABRADOR PENINSULA
ATLANTIC OCEAN
ST. LAWRENCE REGION
CANADIAN SHIELD
INTERIOR PLAINS
PACIFIC COAST REGION
ALASKA
UNITED STATES
Legend
Mesozoic Tertiary
Sedimentary & Volcanic
Intrusives (chiefly granite rocks)
Cretaceous & Jurassic sedimentary formations
Triassic sedimentary & volcanic formations
Intrusives (mostly Diorite)
Paleozoic
Permian
Carboniferous
Devonian
Silurian
Ordovician
Cambrian
Precambrian
Basic intrusives
Acid intrusives (granite, etc.)
Late Precambrian or Early Cambrian
Late Precambrian (Animikie & Keweenawan)
Early Precambrian sedimentary & volcanic formations (Coutchiching, Grenville, Keewatin, etc.)
Undifferentiated (chiefly Archeozoic)
Bureau of Geology and Topography

FIG. 4.

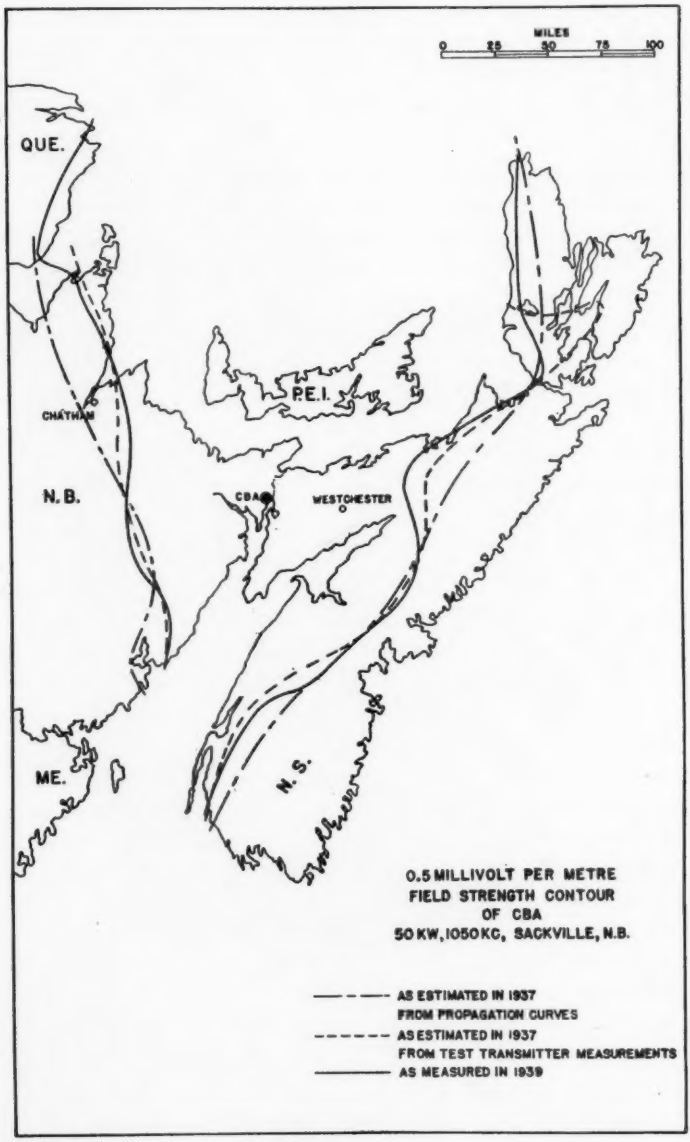
MILES
0 25 50 75 100
QUE.
CHATHAM
P.E.I.
N.B.
CBA
WESTCHESTER
ME.
N.S.
0.5 MILLIVOLT PER METRE
FIELD STRENGTH CONTOUR
OF CBA
50 KW, 1050 KC, SACKVILLE, N.B.
AS ESTIMATED IN 1937
FROM PROPAGATION CURVES
AS ESTIMATED IN 1937
FROM TEST TRANSMITTER MEASUREMENTS
AS MEASURED IN 1939

FIG. 5.

Acknowledgments

This paper is based on an analysis of a great number of field strength measurements taken over a period of years. Up to 1936 all field work was carried out by H. M. Smith, who initiated the program. Since that date, most of the field work has been performed by J. E. Hayes and much of the calculation and analysis by W. G. Richardson. For the able assistance of each of these the author wishes to express his appreciation.

References

1. Burrows, C. R. Bell System Tech. J. 16 : 45-75. 1937.
2. Eckersley, T. L. Proc. Inst. Radio Engrs. 20 : 1555-1579. 1932.
3. Fitch, W. A. and Duttera, W. S. RCA Review, April, pp. 396-413. 1938.
4. Norton, K. A. Proc. Inst. Radio Engrs. 24 : 1367-1387. 1936.
5. Sommerfeld, A. Ann. Physik, 28 : 665-736. 1909.
6. Sommerfeld, A. Ann. Physik, 81 : 1135-1153. 1926.

THERMAL CONDUCTIVITY OF SOME SEDIMENTARY ROCKS[1]

By C. D. Niven[2]

Abstract

The thermal conductivity of some Canadian limestones and slate has been measured. The results are in satisfactory agreement with those of other experimenters, but there was evidence of changes in the stone, even at temperatures below 700° F.; this vitiates the value, from a geophysical standpoint, of these and other determinations.

Owing to the lack of information regarding the thermal conductivity of sedimentary rocks at moderately high temperatures, and the need (2), notwithstanding, of such information in connection with geophysical problems, the thermal conductivities of a number of sedimentary rocks were measured on the high temperature hot plate apparatus in the National Research Laboratories, Ottawa. This apparatus has been described already in connection with an investigation carried out on diatomite bricks (3).

The samples consisted of circular discs of stone 1 in. in thickness and 8 in. in diameter. In determining the thermal conductivity the measurement at the lowest mean temperature was made first, then the temperatures of the plates were allowed to rise until the next mean temperature desired was reached. Usually three mean temperatures are taken in a determination of this sort so that the slope of the curve can be roughly indicated. It was found that the high conductivity of these stones made the determination very much more difficult than it was in the case of a good insulator like diatomite, and the results are therefore given to only one place of decimals. When the work was started it was expected that higher temperatures could be used than those reported, and the first sample that was tested was destroyed by overheating. As, however, a sharp change in the conductivity-temperature curve was observed, it was clear that the determinations below the temperature at which the change in the curve took place were reliable. In the measurement of the conductivity of the other samples, care was taken that the temperature did not exceed that at which the first sample had started to calcine.

It was found that the conductivity fell with rise in temperature; this was somewhat surprising as these stones could not be classed as electrical conductors, and electrical insulators, as a general rule, have higher thermal conductivity at higher temperature. One sample, however, seemed to give results that appeared wrong. Instead of a continuous fall in conductivity with rise in temperature, there appeared to be actually a rise at first, then a fall. When this was discovered, an experimental error was of course suspected

[1] *Manuscript received April 19, 1940.*

Contribution from the Division of Physics and Electrical Engineering, National Research Laboratories, Ottawa, Canada. Issued as N.R.C. No. 918.

[2] *Physicist.*

and a determination at lower temperature was again made. This time a different result was obtained, but this new and lower result did not appreciably help to make the curve continuous. Careful inspection of the original readings taken while the apparatus was coming gradually to thermal equilibrium indicated that the discrepancy in the results was due to a change in the sample, not to any errors in the observations.

After this conclusion had been reached, an examination of previous results showed that the same effect had appeared before, although to a much less marked degree. Presumably, when the stone was heated, a change took place that made the thermal conductivity less than it would have been had the change in the stone not occurred. As the change was accompanied by loss of weight, presumably gas was being expelled at a much lower temperature than that at which the stone started to calcine. The conductivities of the remaining samples that were tested were always measured at the lowest temperature after being measured at the highest. This was always found to be lower than the original determinations at the low temperature, but not always lower than the determination at high temperature. The figures for the various samples are given in Table I and are plotted in Fig. 1.

TABLE I

THERMAL CONDUCTIVITY OF SAMPLES AND LOSS OF WEIGHT DURING TEST

Sample	Density, lb./cu. ft.	Before or during exposure to high temperature test		After exposure to high temperature test		Loss of weight during test, %
		Mean temp., °F.	Thermal conductivity, B.t.u./hr. sq. ft./°F./in.	Mean temp.	Thermal conductivity	
Black Marble "Silvertone Black"	175	256 411 634	10.8 10.5 9.5	243	9.1	0.15
White Marble "Missisquoi White"	172	257 338 461 648	10.0 10.0 10.4 9.6	339	9.1	0.02
Brown Marble "Deschambault Brown"	166	243 385 474 680	11.6 10.5 9.6 7.9			?
Limestone "Rama"	160	266 358 513 711	11.4 11.1 10.6 9.3	246	9.8	0.09
Limestone "Queenston Grey"	167	253 351 490 630	9.9 9.8 9.7 9.2			0.23
Slate	184	248 371 580	10.6 11.4 10.1	251 410 578	10.3 10.2 9.9	0.01

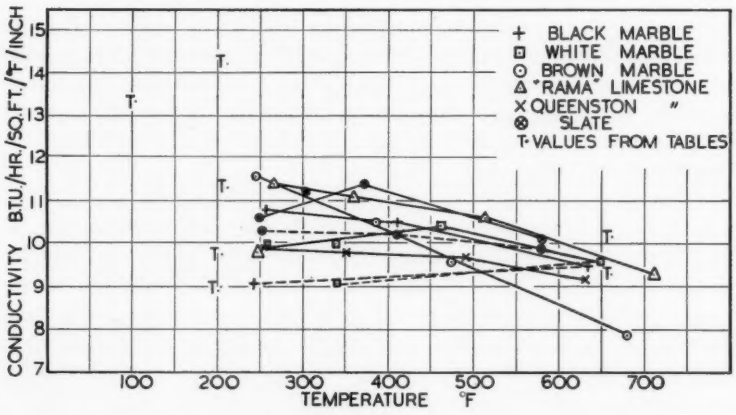

FIG. 1. *Thermal conductivity plotted against temperature.*

Discussion of Results

The data, which are presented in Table I, appear rather puzzling until some facts regarding the composition of the individual samples are considered. It is proposed therefore to discuss each sample individually.

1. *Black Marble*

This sample was obtained from St. Albert, Ont. It is known in the trade as "Silvertone Black", and it contains 96% $CaCO_3$ and some organic matter. Its conductivity gradually fell as higher temperatures were reached; the increase in the rate of fall with rise of temperature was not marked. When the mean temperature was lowered, the conductivity fell slightly, so that the thermal conductivity at low temperature was decidedly lower after heating.

2. *White Marble*

This sample was obtained from Phillipsburg, Que. It is known in the trade as "Missisquoi Marble". It is a very pure calcite and contains little organic matter. Its conductivity rose as the mean temperature was raised, but at higher temperature there was a decided drop in conductivity. When measured again at low temperature after heating, the conductivity was lower than it was at high temperature and very much lower than it had been originally at low temperature. The behaviour of the white marble in this respect rather resembled that of the black marble.

3. *Brown Marble*

This sample was obtained from St. Marc des Carriers, Que. It is known in the trade as "Deschambault Brown ". It is coarse-grained and contains 98% $CaCO_3$ and considerable organic matter such as oils. With rise of temperature, its thermal conductivity decreased more markedly than that of any of the other stones. As this was the stone that was unfortunately overheated, it was impossible to obtain a determination at low temperature after heating.

4. *Buff Limestone*

This sample was obtained from Longford Mills, Ont. It is known in the trade as "Rama". It is a close-grained stone—a mixture of dolomite and calcite—containing 30% $MgCO_3$. Its thermal conductivity decreased quite decidedly with rise in mean temperature. At low temperature, after heating, the thermal conductivity was slightly higher than it had been at high temperature, but very much lower than the conductivity at low temperature before heating.

5. *Bluish-grey Limestone*

This sample was obtained from Queenston, Ont. It is known in the trade as "Queenston Grey", and is a mixture of dolomite and calcite, containing 22% $MgCO_3$. Its conductivity fell fairly steadily as the mean temperature increased, but not to any great extent. Data at lower temperature after heating were not obtained.

6. *Slate*

This sample was obtained from Madoc, Ont. The thermal conductivity at first rose with increase of temperature, then it fell quite markedly. The sample was kept at high temperature for 24 hr. after thermal equilibrium had been reached, and it was found that the thermal conductivity continued to fall slightly. On measuring the conductivity again at low temperature after heating, it was found to be higher than it had been at the high temperature but lower than it was before heating. The behaviour of this sample somewhat resembles the behaviour of the sample of white marble, in that a definite rise in conductivity is shown at first, then a decided decrease as the temperature is raised. As the temperature is lowered, however, the black and the white marble both showed a further fall in conductivity, but the slate showed a small but definite increase. In this respect its behaviour resembles that of the "Rama" limestone. The loss of weight was practically negligible.

General Conclusions

The fact that the change in conductivity is accompanied by a change in density suggests at once that the high temperature drove off a gas and changed the physical properties of the stone to some extent. Such a possibility appears all the more likely when the behaviour of the brown marble is considered. This sample contains quite a considerable amount of organic matter, and, of all the samples, it shows by far the greatest decrease of conductivity with rise of temperature. A comparison of the black and white marbles seems to lend more support to the suggestion, because the black shows a definitely larger decrease in conductivity with rise in temperature than the white: the black, as already pointed out, contains some organic matter. For two reasons, however, it does not seem safe to conclude that the changes in conductivity are due entirely to the driving off of organic matter. In the first place the white marble is a very pure calcium carbonate, and even this stone shows the change, and in the second place some of the stones show a

sort of "recovery" from the effects of heating—as though the gas that was given off was reabsorbed. This is particularly evident in the case of the slate sample, but the "Rama" limestone shows the same phenomenon.

The object of this investigation was to measure the thermal conductivity of the samples, not to determine the effects of heating at moderate temperatures, and a hot plate surrounded with insulation is not a suitable apparatus to use in investigating these effects. That an effect suggesting the driving off of a gas exists, greatly reduces the value of the thermal conductivity measurements, because it means that the data are not exactly applicable to rocks under pressure in the earth. To measure the thermal conductivity of rocks under pressure in the laboratory would be quite a difficult undertaking, and it would require expensive apparatus. The least complicated of all the samples tested was the white marble; the initial rise in conductivity along a line that is nearly parallel to the line representing fall of conductivity after heating suggests that the true conductivity of marble at 650° F. is 10.8 rather than 9.6, but this is a speculation and it cannot be considered as proved. The results of the investigation are accordingly disappointing, as they do not answer accurately the important question, namely, what is the thermal conductivity of sedimentary rocks in the earth at high temperature? All that can be said is that at temperatures between 200° and 700° F., the thermal conductivity of marble, limestone, and slate of density approximately 170 lb. per cu. ft. is about 10 B.t.u. per hr. per sq. ft. per °F. per in. In this respect the results agree very satisfactorily with those of previous investigators. A few points marked *T* in Fig. 1 refer to determinations taken from a table (1). The actual figures are reproduced in Table II. Desvignes, using marble of slightly lower density, obtained a slightly lower conductivity. Poole's results show the definite fall in conductivity with rise in temperature

TABLE II

THERMAL CONDUCTIVITIES DETERMINED BY OTHER INVESTIGATORS

Description of stone	Density, lb./cu.ft.	Mean temp., °F.	Thermal conductivity, B.t.u./hr./sq. ft./°F./in.	Authority
Lerouville hard limestone	159.1	200.8	8.92	Desvignes
Limestone	?	104	13.35	Poole
		104	16.56	Poole
		212	11.32	Poole
		212	14.23	Poole
		662	9.29	Poole
		662	10.16	Poole
Marble	168.9	203	9.00	Desvignes
Grey Belgian marble	168	205	9.75	Desvignes
Slate	?	201	10.37	Lees and Chorlton

that the writer found. Desvignes' result with a hard limestone of much the same density as the "Rama" limestone is a little lower than the writer's for the "Rama" limestone. Lees and Chorlton's value for slate is in satisfactory agreement with the writer's. But in spite of the satisfactory agreement in the figures, the results of the investigation described in this communication indicate that the values obtained both by Poole and by the writer are too low at higher mean temperatures for use in geophysical calculations, since it would be necessary, for such calculations, to use values for rock heated under enormous pressures.

Acknowledgment

The writer wishes to thank Mr. M. F. Goudge, Department of Mines and Resources, Ottawa, for obtaining the samples and for supplying the information regarding the origin and composition of the stones, and the quarry owners who supplied the stones ready cut for the apparatus.

References

1. American Society of Refrigerating Engineers. Report Circular No. 1. Revised to 1924.
2. British Association for the Advancement of Science. Report: Thermal conductivities of rocks. 1938.
3. Niven, C. D. Can. J. Research, 11 : 249-253. 1934.

Canadian Journal of Research

Issued by THE NATIONAL RESEARCH COUNCIL OF CANADA

VOL. 18, SEC. B. JULY, 1940 NUMBER 7

VAPOUR PRESSURES AND BOILING POINTS OF BINARY MIXTURES OF HYDROGEN PEROXIDE AND WATER[1]

BY P. A. GIGUÈRE[2] AND O. MAASS[3]

Abstract

The total vapour pressures of binary mixtures of hydrogen peroxide and water have been measured by means of the static method at 30, 45, and 60° C. over the entire range of concentration. The vapour-pressure–composition curves have been found to exhibit large negative deviations from Raoult's law, but no minimum. A special apparatus and experimental technique were devised that enabled the composition of the vapour to be determined in each case. These data were used to obtain the partial pressures of both components. The values thus found are in good agreement with those calculated from the total vapour pressures by means of the Duhem Margules equation. The activities of water and hydrogen peroxide in their solutions have been calculated and interpreted on the basis of the polarity of the two pure liquids.

The normal boiling point and latent heat of vaporization of the solutions were obtained by extrapolation of the vapour pressure data. The results are important in connection with the distillation of aqueous solutions of hydrogen peroxide.

Introduction

The usual methods of preparation of hydrogen peroxide yield only very dilute solutions. For many technical purposes, as well as for the laboratory preparation of pure hydrogen peroxide, these solutions must be concentrated. In practice the concentration is effected almost exclusively by fractional distillation under reduced pressure in special apparatus (12). Hydrogen peroxide being less volatile than water, the first portions that distil over are richer in the latter component. By this method it is possible to prepare solutions containing as much as 98% of hydrogen peroxide (8). However, all attempts made previously in this laboratory to obtain the pure compound by distillation alone were unsuccessful. It was therefore suspected that a constant boiling mixture was formed as in the case of solutions of ethyl alcohol and water.

The vapour pressure curve of pure hydrogen peroxide has been determined over the temperature range 10 to 90° C. by Maass and Hiebert (11). The purpose of the present investigation was to extend these measurements to

[1] *Manuscript received February 16, 1940.*

Contribution from the Department of Physical Chemistry, McGill University, Montreal, Que.

[2] *Holder of a Bursary (1935–36) and a Studentship (1936–37) under the National Research Council of Canada at the time of this investigation. At present, Research Fellow, California Institute of Technology, Pasadena.*

[3] *Macdonald Professor of Physical Chemistry, McGill University.*

the binary mixtures of hydrogen peroxide and water of various concentrations. The main experimental difficulty arose from the fact that hydrogen peroxide decomposes on heating. For that reason a dynamic method was not accurate enough, and the static method had to be altered. Indeed a mercury manometer could not be used directly since mercury is oxidized by hydrogen peroxide vapours. On the other hand, a knowledge of the composition of the vapour was desirable for solving the various problems in connection with the fractional distillation of these solutions. These conditions were fulfilled by means of an apparatus that combined the static method with that of isothermal distillation. The absolute precision of the vapour pressure measurements was only of the order of 1 mm. of mercury.

Experimental

The apparatus was built entirely of Pyrex glass. As shown in the diagram, Fig. 1, it made use of a glass manometer, *D*, of the spoon type. The flask *A*, of about 100 cc. capacity, was fitted with a ground joint so that it could be easily filled and cleaned after each run. A glass enclosed stirrer was operated by an electromagnet, *S*, in such a way as to break through the surface of the liquid at every stroke. A water thermostat, which could be lowered by means of a pulley and counterweight mechanism, surrounded the flask *A*. The temperature of this water bath was kept constant to 0.1° C.

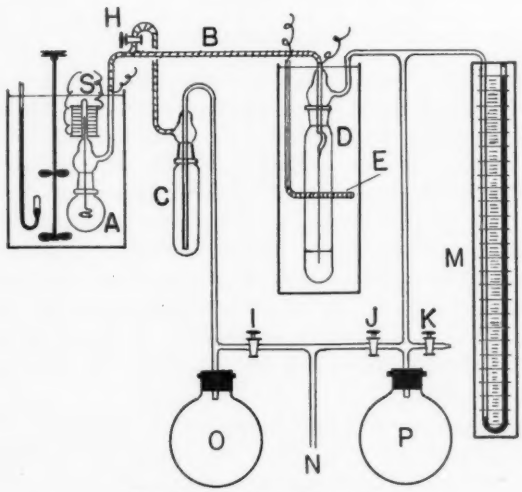

FIG. 1. *Diagram of apparatus.*

The principle and operation of the spoon gauge have been fully described elsewhere (14). With the one used in the present investigation a difference of pressure of about 1 mm. of mercury could be detected. A greater sensitivity was needless in view of the fact that the vapour pressures were not obtained

directly. The glass pointer was observed through a small telescope having a vertical cross-hair. The jacket of the gauge was partly filled with glycerol in order to damp the vibrations of the pointer. The zero point of this system was checked frequently. All parts of the apparatus containing hydrogen peroxide vapour had to be heated to a temperature slightly above that of the thermostat to prevent condensation. For that purpose, the connecting tube, *B*, was wound with Nichrome wire and wrapped in asbestos. The intensity of the current through the resistance wire was controlled so as to keep the tube at about 10° C. above the temperature at which the measurements were carried out. The stopcock *H* on the evacuating tube was connected upward, as shown on the diagram, since it could not be heated directly. The gauge itself was immersed in a water bath made of a battery jar. The upper part only of this water bath was heated by a resistance coil, *E*, so that the image of the pointer would not be distorted by convection currents. The mercury manometer, *M*, was made of 15 mm. tubing, and was equipped with a mirror scale graduated in millimetres. The apparatus was evacuated by a Hyvac pump connected at *N*. A gas trap, *C*, cooled in liquid air, prevented the hydrogen peroxide vapour from reaching the pump or the mercury manometer. This trap was also fitted with a ground joint to allow the vapours that condensed in it to be analysed after each run. The two flasks, *O* and *P*, each of two litres capacity, acted as compensating reservoirs for the pressure and helped in securing a finer adjustment of the gauge. The apparatus was first tested for leaks and a check measurement was made with distilled water. The pure solutions of hydrogen peroxide and water were prepared from commercial 30% Perhydrol by the usual method (8).

The determinations were made as follows: About 50 cc. of the solution of known composition was placed in flask *A*, and the thermostat was heated to the desired temperature. When equilibrium was attained, the whole system was slowly evacuated. First the dissolved oxygen from the decomposition of the peroxide was given off by the liquid, and then, at the pressure corresponding to its own vapour pressure, the solution boiled vigorously. The vapours condensed readily in the liquid air trap, *C*. After a few seconds, stopcocks *I*, *J*, and *H*, were closed. The moment at which the last was closed was recorded by means of a stopwatch. The gauge was then quickly brought back to the zero point by admitting enough air through stopcock *K*. Because of the decomposition of hydrogen peroxide, the pressure increased steadily and the gauge had to be reset every minute or so. The corresponding readings of the manometer were recorded and plotted on a graph against time, as in Fig. 2. Except for the first two or three readings, line *AB*, which were too small owing to the cooling of the solution by evaporation, all values fell quite closely on a straight line, *BC*. Extrapolation of this curve to zero time gave the correct vapour pressure, *D*, of the solution.

Before another set of readings was taken, the space above the solution was exhausted by opening stopcock *H*. The vapours from the boiling solution carried away the oxygen formed during the previous run, so that the true

equilibrium was re-established at the liquid-vapour interface. After three or more such runs had been carried out, the entire system was brought back to normal pressure. The solution was analysed, and after dilution with the suitable quantity of distilled water, it was used for another determination.

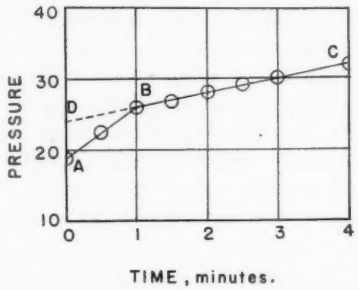

FIG. 2. *A typical run showing the increase of pressure over the solution due to the decomposition of hydrogen peroxide.*

Results

The experimental results of the three series of determinations are given in Table I. The temperature range of these measurements was limited, especially in the case of the very concentrated solutions, by their low vapour pressure below 30° C., and, on the other hand, by the large rate of decomposition of

TABLE I

EXPERIMENTAL RESULTS

Mole fraction H_2O_2		Vapour pressure, in mm.	Mole fraction H_2O_2		Vapour pressure, in mm.
Liquid	Vapour		Liquid	Vapour	
At 30° C.					
0.725	0.270	7	0.225	0.025	23
0.590	0.185	10	0.105	0.005	28
0.475	0.105	13			
At 45° C.					
0.910	0.725	11	0.500	0.090	30
0.870	0.615	12	0.380	0.050	40
0.865	0.590	13	0.290	0.025	47
0.750	0.335	14	0.205	0.010	55
0.600	0.195	23	0.090	0.005	65
At 60° C.					
0.540	0.135	56	0.255	0.030	112
0.435	0.080	71	0.095	0.010	137

hydrogen peroxide above 60°. These results are represented in Figs. 3, 4, and 5. To avoid confusion, a separate diagram was used for each temperature. The upper curve, L, in these diagrams refers to the liquid phase and the lower curve, V, gives the composition of the vapour in equilibrium with the liquid. The curves were drawn on a large scale in order to obtain with a suitable accuracy the values of the vapour pressure at every 0.1 mole fraction interval. These data are tabulated in the first three columns of Table II. The values of the vapour pressure of water given in this table are from the International Critical Tables (5). No redetermination of the vapour pressure of pure hydrogen peroxide was made this time, since the values obtained by extrapolation of the present data for concentrated solutions agree fairly well with those of Maass and Hiebert (11).

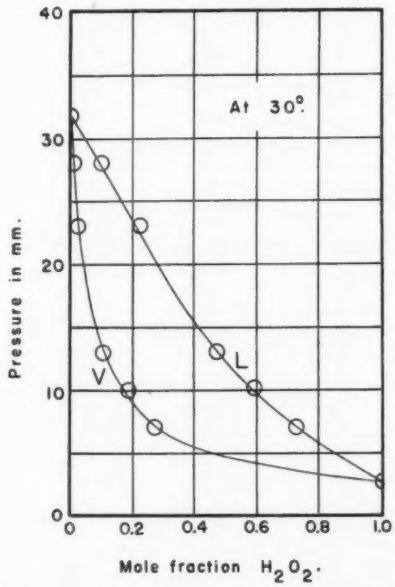

FIG. 3. *Total vapour pressure curves of hydrogen-peroxide–water mixtures.*

From the experimental data on the total vapour pressure and the composition of the vapour, the partial pressures of water and of hydrogen peroxide over their solutions were calculated by means of the equation:

$$p = PN,$$

where P is the total vapour pressure as found by experiment, p is the partial pressure of each component, and N is its mole fraction in the vapour. The values thus found are shown in Table II (fourth and sixth columns). The above method for calculating the partial pressures is open to the objection that the composition of the binary mixture changes during the distillation. In order to minimize that source of error, which assumed a certain importance

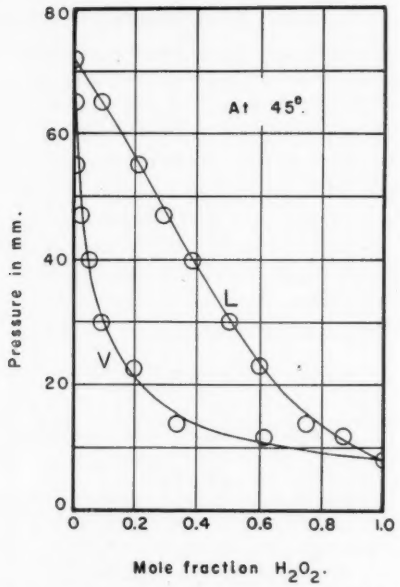

FIG. 4. *Total vapour pressure curves of hydrogen-peroxide–water mixtures.*

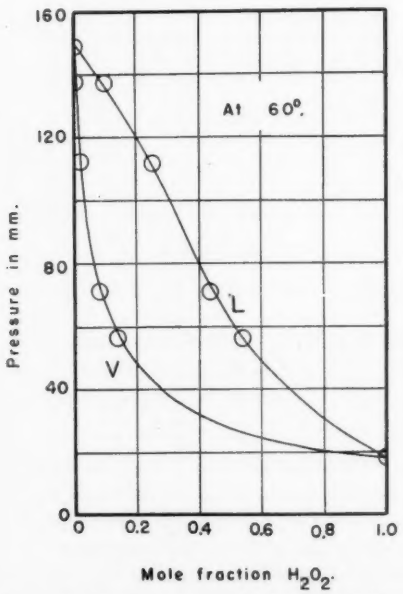

FIG. 5. *Total vapour pressure curves of hydrogen-peroxide–water mixtures.*

TABLE II

TOTAL AND PARTIAL VAPOUR PRESSURES IN THE SYSTEM HYDROGEN-PEROXIDE–WATER

Mole fraction H_2O_2		Total vapour pressure, mm. Hg	Partial pressures, mm. Hg			
			Water		Hydrogen peroxide	
Liquid	Vapour		Found	Calc.	Found	Calc.
At 30° C.						
0.0	0.00	31.82	(31.82)	(31.82)	0.0	0.0
0.1	0.005	28.0	27.85	27.95	0.15	0.05
0.2	0.015	24.2	23.85	24.05	0.35	0.15
0.3	0.03	20.0	19.35	19.66	0.65	0.34
0.4	0.07	15.8	14.75	15.16	1.05	0.64
0.5	0.12	12.3	10.8	11.34	1.5	0.96
0.6	0.18	9.6	7.85	8.34	1.75	1.26
0.7	0.27	7.1	5.2	5.48	1.9	1.62
0.8	0.42	5.2	3.0	3.24	2.2	1.96
0.9	0.68	3.6	1.15	1.12	2.45	2.48
1.0	1.00	2.75	0.0	0.0	(2.75)	(2.75)
At 45° C.						
0.0	0.00	71.88	(71.88)	(71.88)	0.0	0.0
0.1	0.005	64.0	63.7	63.83	0.3	0.17
0.2	0.01	55.4	54.85	54.86	0.55	0.54
0.3	0.025	46.3	45.15	45.23	1.15	1.07
0.4	0.06	38.0	35.7	36.22	2.3	1.78
0.5	0.10	30.0	27.0	27.36	3.0	2.64
0.6	0.175	23.0	18.95	19.34	4.05	3.66
0.7	0.285	16.8	12.15	11.74	4.65	5.06
0.8	0.425	13.2	7.6	7.24	5.6	5.96
0.9	0.705	10.1	3.0	3.08	7.1	7.02
1.0	1.00	7.8	0.0	0.0	(7.8)	(7.8)
At 60° C.						
0.0	0.00	149.4	(149.4)	(149.4)	0.0	0.0
0.1	0.005	137	136.3	136.6	0.7	0.4
0.2	0.01	122	120.8	121.2	1.2	0.8
0.3	0.035	102	98.4	100.0	3.6	2.0
0.4	0.06	79	74.3	75.0	4.7	4.0
0.5	0.11	61.5	54.7	55.3	5.8	6.2
0.6	0.17	48	39.8	39.6	8.2	8.4
0.7	0.27	37	27.0	26.2	10.0	10.8
0.8	0.42	28	16.2	14.5	11.8	13.5
0.9	0.70	22	6.6	5.7	15.4	16.3
1.0	1.00	18.1	0.0	0.0	(18.1)	(18.1)

in the present case owing to the marked difference in volatility of the two components, the volume of the distillate was made small, about 1 cc., as compared with that of the solution, 50 cc. In fact, an analysis of the solution after each determination revealed that in most cases its composition had not changed by more than 2% during the experiment, which was consistent with the degree of accuracy of the measurements. The decomposition of hydrogen

peroxide in the vapour phase was also responsible for a slight inaccuracy in the above method. Therefore it was deemed appropriate to compare the experimental values of the partial pressures with those calculated from the total vapour pressure curves by means of the Duhem Margules equation:

$$\frac{\partial p_1}{\partial N_1} \Big/ \frac{\partial p_2}{\partial N_2} = \frac{p_1}{N_1} \Big/ \frac{p_2}{N_2}.$$

The calculations were made by means of a simplified method (1) for intervals of 0.1 mole fraction. As may be seen in Table II, the agreement between the two sets of figures is satisfactory except for the partial pressure of hydrogen peroxide over its dilute solutions. In these cases, and for the reasons mentioned before, the calculated figures are more reliable than those obtained from the analysis of the vapour. Fig. 6 shows that both components have equal partial pressures when the binary mixtures contain 90% (or 0.82 mole fraction) of hydrogen peroxide.

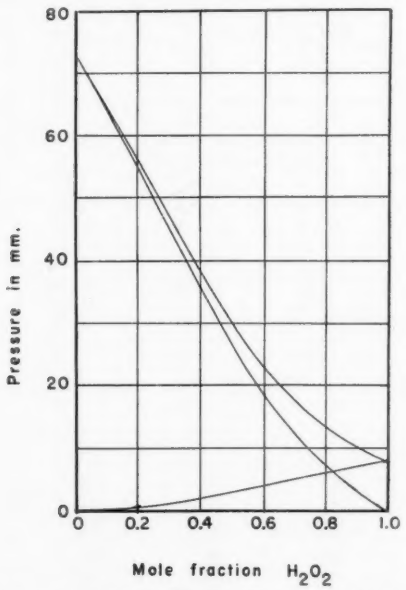

FIG. 6. *Total and partial vapour pressures of water and hydrogen peroxide over their binary mixtures at 45° C.*

By extrapolation of the vapour pressure data at the three temperatures of the measurements it was possible to obtain the normal boiling point of the solutions. The Ramsay and Young rule was used preferably to the logarithmic formula of Rankine. The latter involves three constants that vary independently with the composition of the solutions. The values of the Ramsay and Young constant,

$$K = \frac{T_{\text{solution}}}{T_{H_2O}},$$

are given for the three temperatures in Table III, together with the average values used for calculating the boiling points. In like manner the heat of vaporization of the solutions was calculated by means of the equation:

$$L_{\text{sol.}} = \frac{(T_{\text{sol.}})^2 L_{H_2O}}{K(T_{H_2O})^2},$$

where T represents the boiling points on the absolute scale, and L the molecular heats of vaporization. However, these figures are only approximate owing to the uncertainty of the extrapolation.

TABLE III

BOILING POINT AND LATENT HEAT OF VAPORIZATION OF BINARY MIXTURES OF HYDROGEN PEROXIDE AND WATER

Mole fraction of H_2O_2	Ramsay and Young constant				Boiling point, 0° C.	Heat of vaporization, cal./gm.
	30° C.	45° C.	60° C.	Av.		
0.0	1.000	1.000	1.000	1.000	100.0	(539.5)
0.1	1.006	1.006	1.006	1.006	102.2	498
0.2	1.016	1.015	1.013	1.015	105.6	466
0.3	1.026	1.026	1.025	1.026	109.7	437
0.4	1.039	1.038	1.041	1.039	114.5	414
0.5	1.054	1.052	1.057	1.054	120.1	395
0.6	1.068	1.069	1.073	1.070	126.1	376
0.7	1.085	1.089	1.090	1.088	132.8	362
0.8	1.103	1.106	1.107	1.105	139.2	350
0.9	1.122	1.123	1.123	1.123	145.9	335
1.0	1.135	1.133	1.136	1.135	150.5?	326?

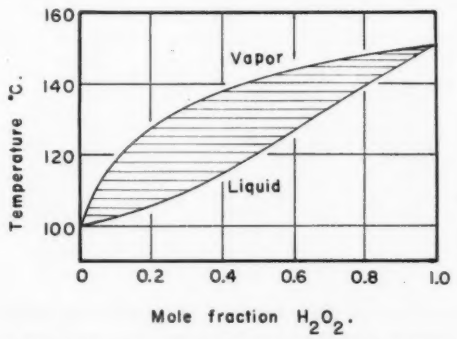

FIG. 7. *Boiling point diagram of the system water–hydrogen-peroxide.*

Discussion

The measurement of the vapour pressures described above has shown conspicuously that the system water–hydrogen-peroxide exhibits large negative deviations from Raoult's law. This is well illustrated in Fig. 8, where the activities or vapour pressure ratios, p/p°, of each component over their binary mixtures at 45° have been plotted against concentration. The two curves

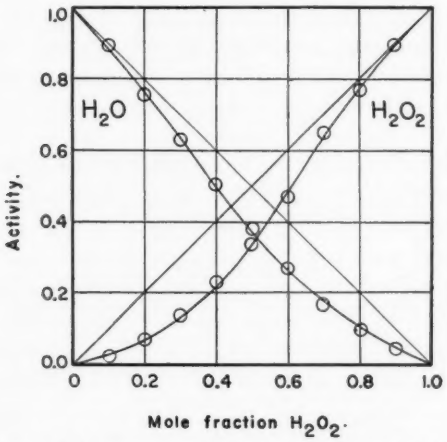

FIG. 8. *Activities at 45° C. of water and hydrogen peroxide over their binary solutions.*

are nearly symmetrical and, at high concentrations, they approach Raoult's law, which is represented by the straight lines. A quantitative measure of the deviations from ideal behaviour is given by the departure from unity of the activity coefficient, γ, which is the activity per molecule. Values of this function for water and hydrogen peroxide at 45° C. were calculated by means of the equation $\gamma = p/p^{\circ}N$, and are given in Table IV.

TABLE IV

ACTIVITY COEFFICIENTS AT 45° C.

Mole fraction of H_2O_2	γ_{H_2O}	$\gamma_{H_2O_2}$	Mole fraction of H_2O_2	γ_{H_2O}	$\gamma_{H_2O_2}$
0.0	1.000	(0.195)	0.6	0.674	0.783
0.1	0.998	0.218	0.7	0.546	0.930
0.2	0.954	0.346	0.8	0.506	0.957
0.3	0.902	0.458	0.9	0.428	1.005
0.4	0.843	0.571	1.0	(0.345)	1.000
0.5	0.761	0.676			

The approximate values of the activity coefficient at infinite dilution, given between brackets, were obtained by plotting log γ against $(N_2)^2$ which gives a straight-line relationship.

The character of these deviations from Raoult's law is consistent with the nature of the two liquids involved (4). Indeed water and hydrogen peroxide are known to be highly polar and associated, the latter being slightly more so. The existence of large permanent dipoles in these molecules is clearly indicated by their high dielectric constant (7). For comparison Table V shows the values of this property and of others indicating the great polarity of the two liquids.

TABLE V

POLARITY DATA FOR WATER AND HYDROGEN PEROXIDE

	H_2O	H_2O_2
Dielectric constant, ϵ at 0°	84.4	93.7
Dipole moment, $\mu \times 10^{-18}$ e.s.u.	1.90	2.13
Heat of vaporization, kcal./mole.	9.71	11.61
Trouton's constant	26.2	27.3
Ramsay and Shields' constant	1.08	0.92

These data place the two liquids in the same order except for the Ramsay and Shields constant, which is based on the surface tension, and is therefore of less relative value in the case of polar liquids. As a consequence of so high a polarity, the attractive forces between the two types of molecules are enhanced, this resulting in a decrease of the escaping tendency and a lowering of the vapour pressure of the solution. Other properties of the solutions also reveal the existence of this interaction. For instance, density measurements indicate that a contraction occurs, as expected, when hydrogen peroxide and water are mixed. The specific volumes of these solutions given in Table VI, together with the decrease of volume, Δv, on mixing, were obtained from the data of Maass and Hatcher (8).

TABLE VI

SPECIFIC VOLUMES OF HYDROGEN-PEROXIDE–WATER MIXTURES

H_2O_2, %	At 0° C.		At 18° C.	
	v	Δv	v	Δv
0.0	1.00015	0.0000	1.0015	0.0000
10.57	0.9598	0.0068	0.9641	0.00455
22.33	0.9179	0.0115	0.9246	0.0078
40.14	0.8580	0.0150	0.86565	0.01165
56.70	0.8062	0.01435	0.8150	0.0113
61.20	0.7930	0.0133	0.8022	0.0101
73.44	0.7566	0.0119	0.76505	0.00945
84.86	0.7226	0.0087	0.7320	0.0072
90.42	0.7070	0.0067	0.7166	0.00544
98.89	0.6851	0.0018	0.69424	0.0016
100.00	0.6834	0.0000	0.6924	0.0000

Likewise the dielectric constant of these solutions has been found to be much greater over a large part of the concentration range than that of either constituent (2). It must be pointed out here that the maximum of these deviations occurs at a different composition of the solution in each case, as is usually true, and that it bears no simple relationship to the composition of any definite compound (15).

The heat of mixing of water and hydrogen peroxide has not so far been measured, but it is known from experience to be positive, in agreement with the negative deviations of the vapour pressure. Although it must be remembered that such calculations have often led to incorrect results, an idea of

the order of magnitude of this quantity may be gained from the values of the partial molal heat of mixing of one component in solutions of various concentrations (Table VII) as calculated from the equation (6): $\Delta H = RT \ln p/p°$.

TABLE VII

PARTIAL MOLAL HEAT OF MIXING AT 20° C. OF WATER AND HYDROGEN PEROXIDE IN THEIR BINARY SOLUTIONS

Mole fraction of H_2O_2	H_2O, cal.	H_2O_2, cal.	Mole fraction of H_2O_2	H_2O, cal.	H_2O_2, cal.
0.1	66	2222	0.6	764	440
0.2	158	1557	0.7	1053	224
0.3	269	1157	0.8	1346	157
0.4	399	861	0.9	1832	66
0.5	563	632			

The formation of the molecular compound, $H_2O_2 \cdot 2H_2O$, as shown by the freezing point curve of this system (10), follows also from the polar nature of the two liquids. Truly enough this compound is much less stable than could be expected from the above considerations. The flatness of the curve at its melting point indicates that this compound is virtually all dissociated in solution. The reason for this peculiarity must be ascribed to the lack of acid and basic character of water and hydrogen peroxide. Confirmation of this explanation is seen in the remarkable stability of the compound $H_2O_2 \cdot NH_3$ (9), despite the fact that ammonia is much less polar than water. The absence of a minimum in the vapour pressure curves may be due to the same cause. The magnitude of the polarity of liquids containing hydroxyl groups is closely connected with the formation of hydrogen bonds. From the heat of sublimation, the energy of the hydrogen bonds has been shown to be about the same in hydrogen peroxide as in water (13).

From the practical standpoint the above results are important in connection with the concentration of aqueous solutions of hydrogen peroxide obtained by distillation. The efficiency of fractional distillation for separating the constituents of a binary mixture depends on the relationship between the composition of the liquid and that of the vapour above it. That relationship in the present case is illustrated in Fig. 9. The marked curvature of the line is caused by the great difference of volatility of the two components. Furthermore, this relationship is not affected appreciably by temperature, as may be seen from the similarity of contour of the three vapour pressure curves, Figs. 3, 4, and 5.

Since the vapour pressure curves show no maximum or minimum, it should be possible to prepare pure hydrogen peroxide by fractional distillation. Calculations based on the ratio of the amount of hydrogen peroxide that distils over to the amount that is left behind show that the efficiency of the distillation decreases very rapidly as concentration proceeds. For instance, when the concentration of peroxide in the solution is 88%, the efficiency is about 50%, but when the concentration reaches 95% the efficiency drops to

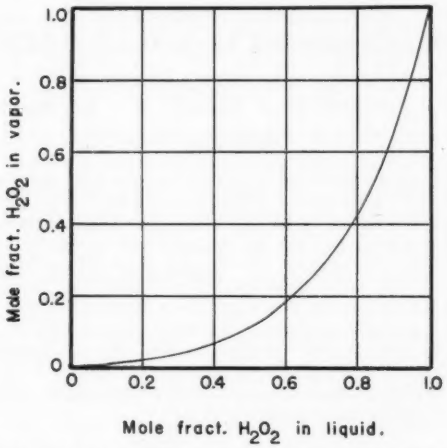

FIG. 9. *Showing the ratio of the concentration of hydrogen peroxide in the solution to that in the vapour above it.*

less than 20%. At this point, however, the rate of decomposition of hydrogen peroxide becomes so important as to counteract fully the effect of the distillation, and no further gain is possible. Slightly higher concentrations, up to 98%, may be obtained by working at lower temperature and pressure in order to reduce the decomposition. However a reasonable balance must be kept between the loss by decomposition and the time required for the operation. Another important consideration is the degree of purity of the final product. It is well known that hydrogen peroxide when heated dissolves glass. This factor becomes important when it is remembered that the final product of the operation in the present case is not the distillate but the residue of the distillation. It may be concluded, therefore, that fractional crystallization, although rather ineffective (3), is actually the only method for obtaining 100% pure hydrogen peroxide.

References

1. BOISSONAS, C. G. Helv. Chim. Acta, 22 : 541-547. 1939
2. CUTHBERTSON, A. C. and MAASS, O. J. Am. Chem. Soc. 52 : 489-499 1930
3. GIGUÈRE, P. A. and MAASS, O. Can. J. Research, B, 18 : 66-73. 1940.
4. HILDEBRAND, J. H. Solubility. 2d ed. Reinhold Publishing Corp., New York. 1936.
5. INTERNATIONAL CRITICAL TABLES. Vol. 3. McGraw-Hill Book Company, New York. 1938.
6. LEWIS, G. N. and RANDALL, M. Thermodynamics. McGraw-Hill Book Company, New York. 1923.
7. LINTON, E. P. and MAASS, O. Can. J. Research, 4 : 322-329. 1931.
8. MAASS, O. and HATCHER, W. H. J. Am. Chem. Soc. 42 : 2548-2569. 1920.
9. MAASS, O. and HATCHER, W. H. J. Am. Chem. Soc. 44 : 2472-2480. 1922.
10. MAASS, O. and HERZBERG, O. W. J. Am. Chem. Soc. 42 : 2569-2570. 1920.
11. MAASS, O. and HIEBERT, P. G. J. Am. Chem. Soc. 46 : 2693-2700. 1924.
12. MACHU, W. Das Wasserstoffperoxyd und die Perverbindungen. Julius Springer, Vienna. 1937.
13. PAULING, L. The nature of the chemical bond. Cornell University Press, Ithaca, N.Y. 1939.
14. PHIPPS, T. E., SPEALMAN, M. L., and COOKE, T. G. J. Chem. Education, 12 : 321-322. 1935.
15. TIMMERMANS, J. Les solutions concentrées. Masson, Paris. 1936.

GELATION PHENOMENA IN WHEAT FLOUR FILMS[1]

By J. D. Hamilton[2]

Abstract

Empirical equations describing the behaviour of wheat protein films studied by means of the hydrophil balance technique are presented. Evidence is given which shows that the protein forms a gel when the film area is decreased and that degelation occurs when the area is expanded. A theoretical picture of gel structure is developed to account for the phenomena characteristic of gelation and degelation. Two major assumptions are used: the protein micelles in the gelled condition and in the film stage are in equilibrium only when the film micelles are close packed and oriented in such a position that the binding force between the film micelles and the aqueous substrate is perpendicular to the water surface. From these assumptions the general form of the gel term is deduced and it is then shown that gels in the form of logarithmic spirals satisfy the physical and theoretical conditions.

The foam created when a wheat flour is shaken with water will spread rapidly over a clean water surface, forming a protein film whose properties may be studied with the aid of the Langmuir hydrophil balance. This article describes an investigation of the properties of films formed by various kinds of flour.

In general, the behaviour of the films is similar to that reported by Hughes and Rideal (3) for films prepared from purified gliadin. Significant differences have been found however in the properties of films formed by flours of different strengths. A mechanism is suggested to account for these differences and for other phenomena that occur during gelation and degelation of the protein.

Procedure

The methods of obtaining quantitative amounts of protein are difficult and uncertain. Films may be formed by spreading from dry protein placed in contact with the water surface or from a protein solution or, as in the present case, from a protein-water foam.

Flour films cannot be formed by placing dry flour in contact with the water surface. The particles of flour drop through the surface to the bottom of the tray. Spreading from solutions would involve preliminary treatment of the flour, and, in addition to the fact that the amount of protein leaving the solution for the film is uncertain, there is also the objection to selective peptization. The formation of films from foam is simple and direct. The spreading takes place very quickly, and by placing enough film on the surface to bring the pressure of the spread film up to an arbitrary value it was found that the form of the curve was reproducible and the characteristics of the phenomena were always the same.

[1] *Manuscript received February 9, 1940.*
Contribution from the Department of Pharmacy, University of Manitoba, Winnipeg, Man.
[2] *Assistant.*

The quantitative error introduced by this method of film formation was apparently not large enough to obscure certain differences between film data obtained with flour blends which formed a series having 10% differences in their hard Canadian and soft English flour fractions. While the present paper does not aim to enquire into the causes of these qualitative differences, their presence is perhaps the best recommendation for the use of the foam method of forming films. Films spread from foam are most likely to be representative of the flours from which they are drawn, for it is now known (1, p. 90) that the process of shaking so as to produce a foam allows the formation of surface films of protein on solutions in which the protein is normally soluble.

No attempt was made to buffer the distilled water used as a substrate, chiefly because of the desire to avoid the possibility of chemical reactions of substrate ions with the protein. However, the singly distilled water may have contained traces of ions, and, since it is now known that very minute amounts of ions can have marked effects on film properties (5), the possibility that these small amounts may have had a role in the phenomena described should not be overlooked.

Two basic procedures were used. If a compression or gelation curve was desired the foam was spread over a previously clean water surface to give the initial area and pressure. The area between the movable barrier and the balance paddle was then diminished and readings of pressure were taken when the film pressure had reached a final equilibrium value. When an expansion or degelation curve was required the film was spread to give the initial area and pressure. It was then compressed into a minimum area, sufficient time was allowed for the pressure to come to equilibrium, and the barrier was then moved outwards. Equilibrium pressure readings were taken for various areas.

Empirical Description of Phenomena

Pre-gelation Phenomena

Both Hughes and Rideal's curves with gliadin and the curves obtained directly with flour show that over a pressure range of from 5 to 14 dynes per cm. of the hydrophil balance float, the force-area curve is linear. This is the range MK indicated in Fig. 1. All points on MK show the pressure to be independent of time, the empirical equation being

$$F_1 = N_1 - M_1A_1 \qquad (1)$$

where F_1 is the force observed when the area is A_1 at any time after the film area has been decreased. The subscript "1" refers to the fact that successive pressure readings were made on a film whose area was being decreased.

The empirical form given in Equation (1) holds for films undergoing compression for a pressure of less than 14 to 15 dynes and areas greater than A_0. A_0 may empirically be defined as 0.64 times the area at which a pressure of 6 dynes is observed.

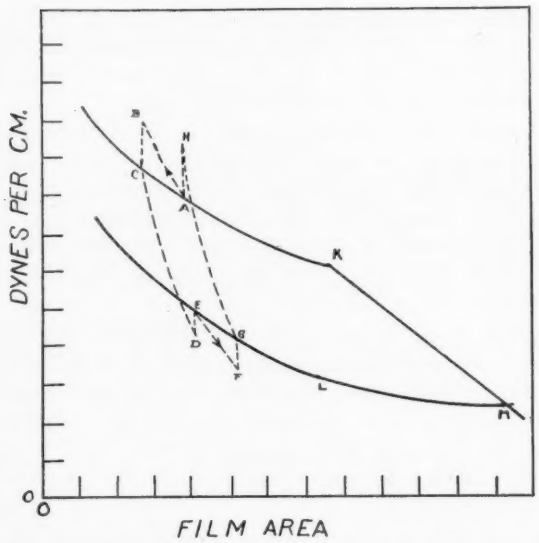

FIG. 1. *A diagrammatic representation of the characteristic phenomena of wheat protein films discussed in the text.*

Gelation Phenomena

When the area is less than A_0 the nature of the phenomena changes. Double values of pressure are obtained, one being observed immediately the area is diminished and the other after a short but variable period of time. Fig. 1 indicates this effect in the points A, B, and C. The pressure instantaneously rises from A to B and then falls from B to C. The upper points B, H lie in what Hughes and Rideal call the metastable state; the lower set of equilibrium points C, A, K are in the gel state.

In the present work, data on the metastable state were difficult to obtain with a hydrophil balance which was ill adapted to taking instantaneous readings of rapidly varying pressures. Consequently, metastable pressures were not investigated and all data refer to the equilibrium points on the gel curve. These were obtained by waiting until it could be reasonably certain that the pressure had ceased falling.

The gelation curve was followed with films from flour up to pressures of 22 dynes per cm. In the higher ranges, striae can easily be seen in the film. These can be removed from the water surface by dipping a microscope slide covered with a rubbed-down coat of ferric stearate through the surface. Photomicrographs of the gels are shown in Fig. 2.

Degelation Phenomena

The gel striae, shown in Fig. 2, disappear on re-expansion of the film. When the area is first increased, the pressure falls from C to D, and then after a short time rises to the degelation pressure F_2 shown at E. The sub-

PLATE I

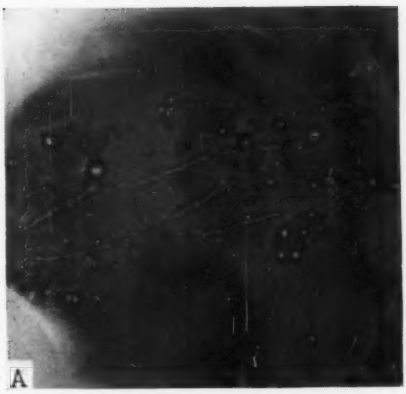

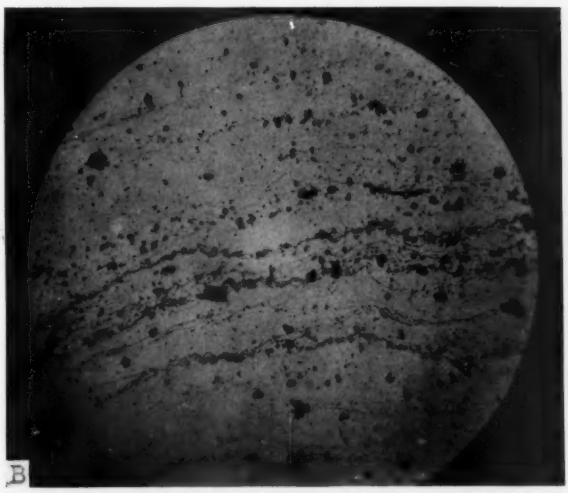

FIG. 2. *Photomicrographs of gelled wheat protein film showing the gel striae and starch clusters and particles. The axes of the striae lie parallel to the barriers of the hydrophil balance. A. ×600. B. ×120.*

script "2" refers to the fact that the film area is being increased. Another increment in area will give a sub-degelation point F and the degelation point G. The locus EG may be plotted from the equilibrium values. At L the film area is the same as that at which gelation first began. Here there is a discontinuity of the slope of the curve. This effect can be seen more clearly in Fig. 3. The exact form of the curve LM is not certain.

It is experimentally possible to repeat a number of cycles $ABCDEFG$ $HABC$ . . . .

Empirical Equations

Plots of three gelation and degelation curves obtained with three flours of different protein content, dough handling, and baking characteristics are

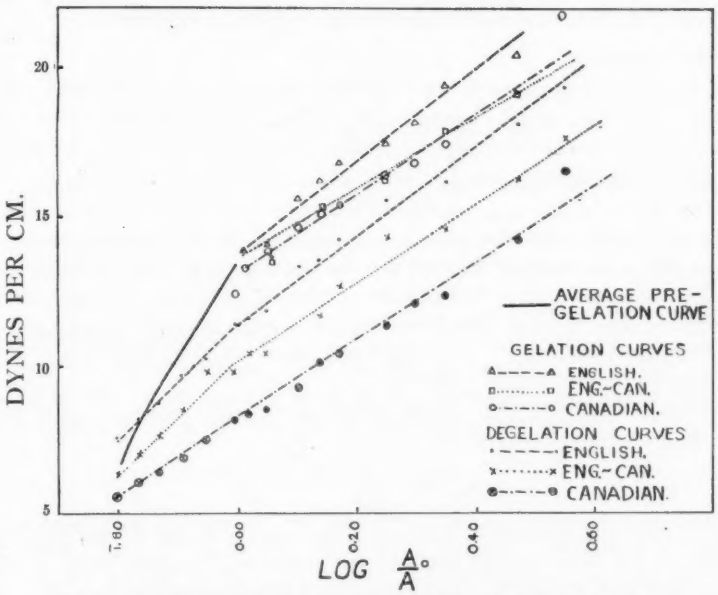

FIG. 3. *Gelation and degelation curves obtained with three different flours.*

shown in Fig. 3. These curves, taken as samples of the data obtained, indicate that the empirical equations for both states are of the same form:

$$F_1 = K_1 + B_1 \log_{10}\left(\frac{A_0}{A_1}\right) \tag{2a}$$

$$F_2 = K_2 + B_2 \log_{10}\left(\frac{A_0}{A_2}\right) \tag{2b}$$

Formulation of a Picture of the Gelation and Degelation Processes

Pre-gelation State

From considerations of the pressure and film potential changes during compression of gliadin films in the pre-gelation stage, Hughes and Rideal sug-

gested that a rearrangement of both the residue groups and the polypeptide chains or lattices takes place. Initially the residues, which have some slight hydrophilic tendencies, and the strongly hydrophilic lattices are lying in the water surface. As the available surface area is diminished, the residues leave the surface and assume a more or less perpendicular position. This allows the protein micelles to form a close packed film. Thus when the critical area A_0 is reached, the film is composed of close packed micelles that are occupying their minimum area and have marked dorsi-ventral differences. K_1 may be physically interpreted as the maximum peripheral pressure that the micelles develop before gelation begins. It is assumed that a further decrement in film area crowds the micelles to such an extent that they buckle and are tipped out of their surface orientation and take on a new type of orientation represented by the logarithmic term in the empirical equation.

Metastable Pressure

The metastable pressure is very probably the result of the tilting of the micelles. For if R_n is the normal binding force of the polypeptide surface to the water, then the tilting will result in an increase in the observed horizontal pressure by an amount

$$R_n \cos \alpha . \tag{3a}$$

This metastable pressure can be written in a more complete form. Let N_{max} be the total number of micelles that can be accommodated in a unit area of surface under the close packed condition. Now let the decrement in film area be ΔA, so that the decrement in a unit area Δa will be $\Delta A/A_1$. This decrement Δa results in a temporary increase ΔN_e in excess of N_{max}. These are accommodated by tilting.

From these considerations the maximum metastable pressure can be placed in two forms. The first of these,

$$R_n \Big/ 1 + \frac{A_1}{\Delta A} , \tag{3b}$$

indicates that as the area is decreased the disorientation of the micelles in the film stage is more marked and the metastable increase over the gel pressure is greater. This is due to the fact that the area decrement is distributed over a smaller number of micelles.

The second form

$$R_n \Delta N_{e_{t-t}} \Big/ \left(N_{max} + \Delta N_{e_{t-t}}\right) \tag{3c}$$

is obtained by expressing $\cos \alpha$ in terms of ΔN_e and including the time dependent decrease of the excess micelles as

$$\Delta N_{e_{t-t}} = \Delta N_{e_{t=0}} \varphi(a_1 , t) , \tag{4}$$

where $\Delta N_{e_{t-t}}$ is the number of micelles per unit area in excess of N_{max} at a time t following the area decrease. Also $\varphi(a_1 , t)$ is a function of a parameter a_1 and the time t. It is known to be rapidly convergent with an initial condition $t = 0$, $\varphi = 1$, and a final condition $t = \infty$, $\varphi = 0$.

General Form of the Gel Term

The fall in metastable pressure expressed by Equation (3*c*) is accompanied by a rise in the gel pressure. ΔN_g micelles leave the film and enter the gel. Thus:

$$\underset{t-t}{\Delta N_g} = \underset{t-o}{\Delta N_c} (1 - \varphi(a_1,t)) . \tag{5}$$

It is clear from considerations given above that A_0 in Equations (2*a*) and (2*b*) is related to N_{max} as

$$N_{max} = \frac{\text{const.}}{A_0} \tag{6a}$$

and A_1 and A_2 are related to the number of micelles N_g that have entered the gel. That is

$$N_g = \frac{\text{const.}}{A_0 - A} \tag{6b}$$

Therefore the empirical equations must take the form

$$F = K + B \log \left(\text{const.} \frac{N_g}{N_{max}} \right) . \tag{7}$$

Other consideration must be given to this logarithmic function. The gel pressures observed are associated with a force that is acting perpendicular to the longitudinal axis of the gel striae, as can be seen in Fig. 2–*B*. The force is associated with the structure and size of the gel cross-sections, which are presumably more or less circular.

Physical Possibility of Gel Spirals

One function that satisfies these conditions is the logarithmic spiral $\ln r = a\theta$, where r, θ are the polar co-ordinates of the spiral and a is a constant. The transformation from the empirical equations is effected by

$$B \log_{10} \left(\frac{A_0}{A} \right) = a\theta = \ln r. \tag{8}$$

Before developing the theoretical form of the gel spiral it will be necessary to consider the several possibilities in spiral structure. These are shown in Fig. 4. These spirals can be compared to the protein multi-layers built on stearate glass foundation by the Blodgett technique. Blodgett (2) and Langmuir *et al.* (4) state that if the film is applied on the down trip of the slide, the residue groups lie innermost to the stearate. This is an *A* layer. If the layer is applied on the up trip, a *B* layer results with the polypeptide surface lying innermost.

Two types of multi-layers have been obtained. The first type consists of *B* layers only, the sequence being stearate *B*, *B*, *B*, ... or putting *B* as *RP* with *R* for the residue and *P* for the polypeptide, the sequence is stearate, *PR*, *PR*, *PR*, ... By comparison Spirals (*a*) and (*b*) in the figure are seen to be similar. The uppermost layer in a film of this type does not return to the water surface when the plate is redipped, and if the comparison is valid, one would expect that Spirals (*a*) and (*b*) would not give rise to a reversible gelation.

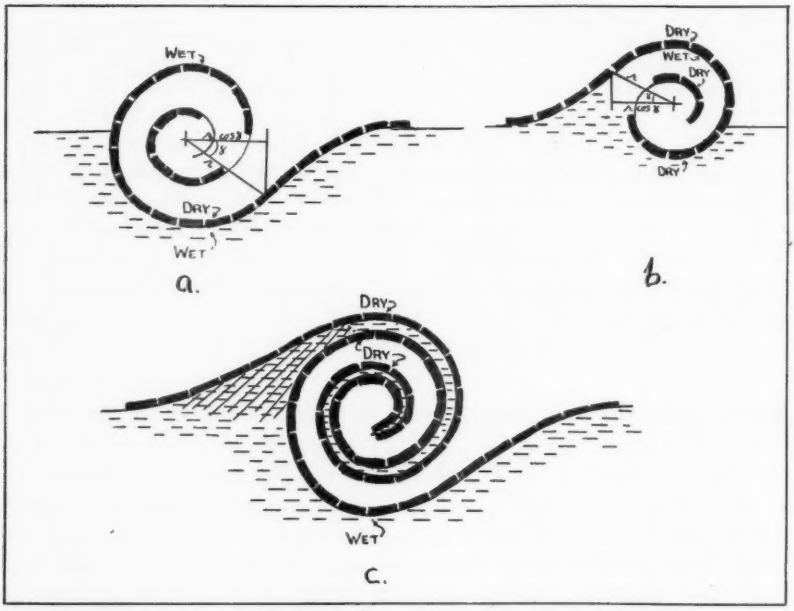

FIG. 4. *Logarithmic spiral cross-sections of gels. The protein micelles are represented as being close packed and oriented with their hydrophilic (wet) polypeptide surfaces toward the substrate and the relatively non-hydrophilic (dry) residue surfaces away from the water.*

There are other reasons for rejecting these spiral types. In (*a*) the hydrophobic residue groups lie outermost at all points. This would cause the gel to float high, and if the gel pressure is proportional to log r, the effective horizontal component would be log ($r \cos \gamma$) as shown. In (*b*) an opposite effect is true. The hydrophilic groups lie outermost at all points and the gel would tend to be dragged under the water surface.

The third spiral (*c*) is similar to the second protein multi-layer structure. When a stearate prepared slide is first dipped through the film, an *A* layer is deposited and as the slide is withdrawn, a *B* film is placed on top of the *A* film. This gives—stearate, *A*, *B*, or stearate, *RP*, *PR*. Here the water is trapped between the *P*, *P* surfaces, and the *RP*, *PR* . . . relationships in Spiral (*c*) are similar to those in this multi-layer. Further, in this multi-layer only two film layers can be deposited, since, on redipping, the *B* layer returns to the water surface. This is comparable to the degelation phenomena; the continued *RP*, *PR*, *RP* . . . relationships in the double gel arise from the continuous manner in which the gel grows. A number of layers *ABABAB* . . . . can be built into multi-layers on the addition of traces of inorganic ions, notably zinc chloride, to the aqueous substrate, and the effect of these ions upon gel stability might possibly throw more light on the validity of the comparison.

The spiral (*c*) satisfies all the conditions of reversibility and continuous growth and it remains to be shown that its formulation is essentially similar to Equation (7).

Gelation Term

If the micelles occupy the same area in the gelled state as they did in the film, then the total length of the double spiral may be taken as equal to $\frac{kNg}{2N_{max}}$. This may be equated to the line integral of the spiral and the result solved for r. The time dependent increase in the spiral gel [Equation (5)] may also be included. The expression obtained is

$$\ln \left\{ \left(\frac{a^2}{1 + a^2} \right)^{\frac{1}{2}} \frac{k}{2} \left(\frac{N_g + \underset{t-o}{\Delta N_g}}{N_{max}} \right) \cos \gamma_1 \right\} , \tag{9}$$

where $\cos \gamma_1$ is a factor whose significance will be discussed below. This is in the form required by Equation (7).

The complete gelation equation may be now written as:

$$F_1 = K_1 + R_n \frac{\Delta N_e}{N_{max} + \Delta N_e} + \ln \left\{ \left(\frac{a^2}{1 + a^2} \right)^{\frac{1}{2}} \frac{k}{2} \left(\frac{N_g + \underset{t-o}{\Delta N_g}}{N_{max}} \right) \cos \gamma_1 \right\} \tag{10}$$

Essential Difference Between Gelation and Degelation

The cycle *ABCDEFGH* indicates that the physical mechanism responsible for the abrupt changes *CD* and *GH* should be sought in the gel and not in the film micelles. The physical interpretation is that the gel does not cut the water surface so that the pressure measured by the hydrophil balance is strictly log r, but in such a position that the pressure is the logarithm of the resolved component of r: log ($r \cos \gamma_1$), log ($r \cos \gamma_2$). When the movable barrier of the apparatus is moved outwards, the sudden increase in area not only allows degelation to begin but also allows a water pressure effect to take place in the cross-hatched region indicated in Fig. 4-*c*. The gel thus tends to enter the water and $r \cos \gamma_1$ is reduced to $r \cos \gamma_2$. Complete immersion is prevented by other features of the double gel. It is this effect that accounts for the dissimilarity in the gelation and degelation curves.

The Sub-degelation Pressure

As in gelation, so too in degelation, the size of the gel is the determining factor in the pressures above some lower limiting value K_2.

In degelation, the increase in area Δa creates a deficiency ΔN_d micelles per unit area. If ΔN_{dg} is the number of micelles that have left the gel and re-entered the film stage at time t then

$$\underset{t-t}{\Delta N_d} = \underset{t-o}{\Delta N_d} \varphi(a_2 , t) \tag{11a}$$

$$\underset{t-t}{\Delta N_{dg}} = \underset{t-o}{\Delta N_d} (1 - \varphi(a_2, t) \tag{11b}$$

This temporary deficiency in the film is reflected in the sudden drops in film pressure *ED* and *GF* in Fig. 1. The drops can be expressed by

$$-\frac{\partial F_2}{\partial N}\Delta N_{\substack{d \\ t-t}}. \tag{12}$$

The Degelation Pressure

The gel term can be expressed in terms of N_g, the number of micelles in the gel. It is shown as the last term in Equation (13).

The Constant K_2

The phenomena of degelation will continue until all the protein has left the gel. For film areas of less than A_0 it is not possible for the film to be other than close packed when the degelation pressure is at its final equilibrium value. But when $A = A_0$, micelles can begin separation and from this it is to be expected that A_0 will be a critical point in degelation phenomena. K_2 may be defined as the pressure obtained when $A_2 = A_0$.

The completed degelation equation is

$$F_2 = K_2 - \frac{\partial F_2}{\partial N}\Delta N_{\substack{d \\ t-t}} + \ln\left\{\left(\frac{c^2}{1+c^2}\right)^{\frac{1}{2}}\frac{k}{2}\left(\frac{N_{\substack{g \\ t-o}} - \Delta N_{\substack{dg \\ t-t}}}{N_{max}}\right)\cos\gamma_2\right\} \tag{13}$$

Post Degelation Phenomena

When the area is greater than the critical area A_0 the nature of the phenomena again changes. This is the portion *LM* of Fig. 1. The form of the equation and the interpretation of the phenomena are not known.

The Time Functions $\varphi(a_1, t)$ *and* $\varphi(a_2, t)$

Apart from their convergency nothing is known about these functions. A thorough investigation into the time factors should yield much valuable information regarding the influence of chemical agents on gelling phenomena.

Acknowledgments

The author wishes to thank Mr. T. R. Aitken of the Board of Grain Commissioner's Research Laboratory for the graded series of flour samples used in this investigation and for the use of laboratory space. He also wishes to express his sincere thanks to Prof. G. O. Langstroth for his criticism and help in the development of the mathematical formulation.

References

1. Adam, N. K. The physics and chemistry of surfaces. 2nd ed. Oxford University Press. 1938.
2. Blodgett, K. B. J. Am. Chem. Soc. 57 : 1007-1022. 1935.
3. Hughes, A. H. and Rideal, E. K. Proc. Roy. Soc. London, A, 137 : 62-77. 1932.
4. Langmuir, I., Schaeffer, V. J., and Wrinch, D. M Science, 85 : 76-80. 1937.
5. Rideal, E. K. and Mitchell, J. S. Proc. Roy. Soc. London, A, 159 : 206-228. 1937.

THE KINETICS OF THE DECOMPOSITION REACTIONS OF THE LOWER PARAFFINS

VI. ETHANE[1]

By E. W. R. Steacie[2] and Gerald Shane[3]

Abstract

The kinetics of the thermal decomposition of ethane have been investigated by the static method in the temperature range 565° to 640° C. The reaction was found to be uninfluenced by surface. The rate of the reaction can be expressed by

$$\log_{10} k = 14.02 - \frac{69700}{2.3RT} \text{ sec.}^{-1}$$

The products of the reaction are ethylene, hydrogen, and a small amount of methane and probably higher hydrocarbons.

The reaction is discussed from the point of view of free radical mechanisms, and it is suggested that the results cast serious doubt on the validity of the Rice-Herzfeld mechanism and its modification by Küchler and Theile.

Introduction

The ethane decomposition has become one of the more important gas reactions on account of its bearing on the role of free radicals in thermal reactions. From this point of view many investigations have been made of the thermal and photochemical reactions of ethane. (For a comprehensive review of the literature see (23).) In view of the uncertainties which still exist concerning the thermal reaction, it has been considered advisable to extend our work on the kinetics of the decomposition reactions of the lower paraffins (26, 27, 35, 36, 37) to ethane.

Early work on the decomposition of ethane by Pease (13) and by Frey and Smith (6) indicated that the reaction led predominantly to ethylene and hydrogen, and that it was homogeneous and probably of the first order. The first reasonably thorough investigation was that of Marek and McCluer (11) who concluded that the reaction was of the first order. Recalculation of their results by Paul and Marek (14) led to the equation

$$\log_{10} k = 16.06 - \frac{77700}{2.3RT} \text{ sec.}^{-1}$$

There is no doubt that their value of the activation energy is not very accurate on account of the non-uniformity of the temperature of their reaction vessel.

A more thorough investigation of the kinetics of the reaction by the static method led Sachsse (19) to the conclusion that the high-pressure rate constants were given by:

$$\log_{10} k = 14.1 - \frac{69800}{2.3RT} \text{ sec.}^{-1}$$

[1] *Manuscript received February 22, 1940.*

Contribution from the Physical Chemistry Laboratory, McGill University, Montreal, Canada, with financial assistance from the National Research Council of Canada.

[2] *Director, Division of Chemistry, National Research Laboratories, Ottawa, Canada. At the time, Associate Professor of Chemistry, McGill University, Montreal, Que.*

[3] *Demonstrator in Chemistry, McGill University.*

He also found that, in addition to ethylene and hydrogen, a certain amount of condensable products was formed. This conclusion is confirmed by the work of Storch and Kassel (38).

Further work on the reaction, including investigations up to higher pressures, was done by Dintzes, Zharkova, Zherko, and Frost (4), Dintzes and Frost (1, 2, 3), and by Travers and his collaborators (40, 41, 42, 43). None of these investigations permits an accurate estimation of the activation energy.

Rice and Herzfeld (15) suggested that the reaction, in common with many other organic decompositions, could be explained on a free radical basis. The main steps postulated were:

		Activation energy, Kcal.
(1)	$C_2H_6 \longrightarrow 2CH_3$	80
(2)	$CH_3 + C_2H_6 \longrightarrow CH_4 + C_2H_5$	20
(3)	$C_2H_5 \longrightarrow C_2H_4 + H$	49
(4)	$H + C_2H_6 \longrightarrow C_2H_5 + H_2$	17
(6)	$H + C_2H_5 \longrightarrow C_2H_4 + H_2$ or $\longrightarrow C_2H_6$	Small

plus various recombination reactions.

Assuming the activation energies listed above, they showed that with certain reasonable assumptions this scheme leads to a first order rate, and to an activation energy for the over-all reaction given by

$$E_{over\text{-}all} = \tfrac{1}{2}(E_1 + E_3 + E_4 - E_6)$$
$$= 73 \text{ Kcal.},$$

in good agreement with the experimental value of Marek and McCluer (11).

Patat and Sachsse (12, 18), however, showed, by means of the ortho-para hydrogen conversion, that the concentration of atomic hydrogen in the system is much less than that predicted by the Rice-Herzfeld mechanism. Furthermore, direct measurement of the value of E_4 by Steacie and Phillips (31, 32), and by Trenner, Morikawa, and Taylor (44) shows that the value assumed by Rice and Herzfeld is much too high. With the new value, about 9 Kcal., the scheme no longer predicts a first order rate.

Furthermore, work on the reactions of hydrogen atoms with ethane (22, 44), and on the mercury photosensitized reactions of ethane (24, 33, 34) suggested that the reaction

$$(7) \quad H + C_2H_6 \longrightarrow CH_4 + CH_3$$

was faster than Reaction (4). The occurrence of this reaction would completely upset the Rice-Herzfeld scheme. It has been suggested by Taylor (39), however, that the facts can be explained without the postulation of (7), provided we assume the occurrence of

$$(8) \quad H + C_2H_5 \longrightarrow 2CH_3 .$$

This assumption is strongly supported by recent work on the reaction of hydrogen atoms with propane (29, 30), and butane (25). It has also received theoretical support (7, 16).

There is some evidence that the decomposition of ethane can be sensitized by free radicals. It is, however, somewhat inconclusive (5, 20). There is also evidence which points to the inhibition of the ethane decomposition by added nitric oxide (8, 21). This indicates a mean chain length of about 12 at 620° C.

The above discussion indicates that while there is considerable indirect support for the idea that free radicals participate in the ethane decomposition, there is little doubt that the mechanism proposed by Rice and Herzfeld is untenable. A recent investigation by Küchler and Theile (10), however, has made a fundamental change in the situation.

Küchler and Theile re-investigated the thermal decomposition of ethane, and found an activation energy of 77 Kcal. They conclude that the free-radical mechanism can be reconciled with the experimental data by assuming that the initial step is bimolecular rather than unimolecular, and that the chains are terminated by the recombination of two ethyl radicals instead of by the union of an ethyl radical and a hydrogen atom as originally suggested by Rice and Herzfeld. Rice and Herzfeld (17) have discussed their mechanism in detail. The success of this mechanism depends on the high value of the activation energy of the over-all reaction (77 Kcal.), which is only slightly below the value assumed by Rice for the activation energy of the initial bond split (80 Kcal.). It therefore seemed worth while to make an accurate re-investigation of the ethane decomposition, with special emphasis on the determination of the activation energy of the reaction.

Experimental

The static method was used so as to permit accurate temperature control, and to enable the investigation of the effect of pressure on the rate of the reaction. A very large reaction vessel was used, however, so that sufficient products were available for analysis. At the same time this made it possible to reduce surface effects to a minimum.

The apparatus was similar to that previously described (35). The reaction vessel was a translucent quartz cylinder of about 15 litres capacity. It was connected through a graded seal to a capillary mercury manometer, and through a stopcock to a storage vessel, pumps, etc. A smaller transparent quartz vessel of 750 cc. capacity was also used in a few runs. The manometer was wound with nichrome wire and heated electrically to prevent condensation of the decomposition products.

The reaction vessel was heated by an electric furnace. This consisted of a three-foot length of 8-in. internal diameter cast iron sewer pipe, with a wall thickness of about one inch. This was surrounded by a set of eight heaters, made by winding 18 gauge nichrome wire on transite strips. These were insulated from the pipe by a thin layer of asbestos paper. The pipe and heaters were surrounded by a layer of pulverized asbestos about 10 in. thick. The reaction vessel was roughly thermostated so as to maintain approxi-

mately the desired temperature between runs. During a run the temperature was manually controlled.

The temperature of the reaction vessel was measured by a set of three chromel-alumel thermocouples in various positions, together with a Cambridge thermocouple potentiometer. The temperature, as measured by any one thermocouple, could be controlled to within $\pm 0.5°$ C. The temperature gradient along the furnace was less than 1° C., and the variation from the centre to the side was about 0.5° C.

Samples of gas were withdrawn for analysis by expansion into an evacuated bulb. The sample was then transferred by means of a Toepler pump to a portable mercury gas holder, and analysed by low-temperature fractional distillation in an apparatus of the Podbielniak type. Analyses were also made by the usual absorption methods in a Burrell gas analysis apparatus.

Ethane was obtained in cylinders from the Ohio Chemical and Mfg. Co. It was stated to be 97% pure. Analysis showed it to contain 1.3% of ethylene, less than 0.3% of hydrogen plus methane, and less than 0.3% of higher hydrocarbons. The cylinder gas was purified by passage through a 50 cm. tube containing copper oxide at 300° C., through saturated bromine water into a two-litre bottle illuminated by a Point-o-lite lamp, through a 40% solution of potassium hydroxide, and finally through a trap at −80° C. to remove water. The gas was then condensed with liquid air into a metal cylinder of about 500 cc. capacity. The needle valve on the cylinder was then closed and the cylinder allowed to warm up. In this way it was possible to purify and store the entire contents of a style *B* cylinder at one time. The resultant gas contained no impurities which could be detected with the analytical methods used.

Results

Calculation of Rate Constants

The main difficulty in the investigation of the decomposition of ethane is that the equilibrium in the predominant reaction

$$C_2H_6 \rightleftarrows C_2H_4 + H_2$$

is far over on the decomposition side only at temperatures so high that the rate of reaction is too high to be conveniently measurable. At the temperatures at which rate measurements can be carried out, equilibrium corresponds to only about 5 to 15% decomposition. As a result the back reaction is a serious complication.

There are two ways to overcome the complication, *(a)* the use of initial rates of reaction, since at the start there will be no back reaction, and *(b)* the expression of the velocity constant of the reverse reaction in terms of the constant for the decomposition reaction and the equilibrium constant. The differential equation for the rate can then be integrated, and the velocity constants calculated by fitting the equation to the data for each experiment.

In the present investigation both methods were used. To lessen the amount of computation involved in the second method, however, the following procedure was used:

In the case of "irreversible" reactions the usual method is to measure the time-to-half-value, or to some other arbitrarily chosen amount of reaction. These times can then be plotted, averaged, etc. The velocity constants can then be obtained from the averaged values by a simple calculation. In the case of a reversible reaction, it can be shown that a simple relation exists between the velocity constant of the reaction, and the time for the reaction to proceed to a certain fraction of the value at equilibrium. We can thus record the data in the form of the time to one-half the equilibrium value, one-quarter the equilibrium value, etc., and calculate the velocity constants from smoothed curve data of this sort in a simple way.

For the main reaction in the decomposition of ethane we have

$$-\frac{d}{dt}(C_2H_6) = K(C_2H_6),$$

and for the reverse reaction

$$-\frac{d}{dt}(C_2H_6) = K^1(C_2H_4)(H_2).$$

Let the initial concentration of ethane be a, the amount reacted at time t be x, and the amount reacted at equilibrium be e. Then at time t we have

$$\frac{dx}{dt} = K(a - x) - K^1x^2. \tag{1}$$

At equilibrium

$$K(a - e) = K^1e^2,$$

or

$$K^1 = \frac{K(a - e)}{e^2}.$$

Substituting for K^1 in (1),

$$\frac{dx}{dt} = K\left(a - x - \frac{(a - e)}{e^2}x^2\right).$$

or

$$\int \frac{dx}{\frac{(a - e)}{e^2}x^2 + x - a} = -Kt + I,$$

where I is a constant of integration. Integrating, we have,

$$\frac{e}{2a - e}\ln\frac{(a - e)(x - e)}{(a - e)x + ae} = -Kt + I.$$

And, evaluating the constant of integration in the usual way by putting $x = 0$ when $t = 0$, we obtain

$$Kt = \frac{e}{2a - e}\ln\frac{(a - e)x + ae}{(e - x)a}. \tag{2}$$

Now if we define t_{25} in this case as the time to reach one-quarter the equilibrium value, then $t = t_{25}$ when $x = e/4$. Hence we have

$$Kt_{25} = \frac{e}{2a - e} \ln \frac{5a - e}{3a}. \tag{3}$$

Note that for an irreversible reaction, i.e., $e = a$, this reduces to the usual relation $Kt_{25} = \ln 4/3$.

For values of e between $0.1a$ and $0.2a$, which is the normal experimental range, we can take an average value of $5a - e$, and to within an accuracy of 2% write

$$Kt_{25} = 0.482 \frac{e}{2a - e}. \tag{4}$$

It follows that from t_{25}, knowing the equilibrium dissociation (or determining it in each run by allowing the reaction to go to completion), we can calculate the value of Kt_{25} very simply from (4), and thus get K.

Similarly, we may use the time to one-eighth equilibrium, and obtain instead of (4), the approximate relation

$$Kt_{12.5} = 0.239 \frac{e}{2a - e}. \tag{5}$$

As will be seen later, the values thus obtained are in excellent agreement with those calculated from initial rates.

The Effect of Surface

The surface-volume ratio of the large reaction vessel was approximately 2.5 times smaller than that of the small vessel. No difference in the rate of reaction was detectable, and it may therefore be concluded that, contrary to the findings of Travers and his co-workers, surface plays no appreciable part. In any case, the conditions with the large vessel were exceptionally favourable for the investigation of the surface-free reaction, on account of the relatively very small surface-volume ratio.

The Reaction Rate

In all about 200 runs were made. In arriving at averages, or smooth curve values of rate constants, etc., the data of all runs were used. The values given in the tables below represent the data of a representative group of runs, chosen to show the magnitude of the experimental uncertainties. The spread in values of the rate constant for runs under identical conditions is relatively larger than is the case with many other reactions. This is due to the fact that at low temperatures where the reaction is slow and time measurements are accurate the equilibrium is so far over on the ethane side that completion corresponds to a very small amount of reaction. On the other hand, at high temperatures, where the equilibrium is more towards dissociation, the reaction is so fast that rate measurements are difficult. As a result the error in an individual run is rather large. However, a large number of runs were made, and the average values should be reasonably reliable.

Rate data from initial rates for representative experiments are given in Table I.

TABLE I

REACTION RATE DATA

Temp., °C.	Initial press., cm.	$K \times 10^4$, sec.$^{-1}$	Temp., °C.	Initial press., cm.	$K \times 10^4$, sec.$^{-1}$
565	41.9	0.79	607	57.2	5.3
	38.0	0.62		38.9	4.8
	34.5	0.63		38.5	4.8
	33.3	0.61		35.1	5.0
	22.4	0.46		31.9	5.0
	18.8	0.68		30.6	5.0
	14.1	0.47		12.1	5.8
572	50.1	1.04	616	62.5	7.5
	48.2	0.67		57.0	7.4
	45.3	0.88		44.6	7.4
	41.0	0.96		26.4	7.5
				16.9	7.8
580	70.9	1.03			
	65.3	1.25	625	51.9	10.0
	50.4	1.16		45.8	11.0
	48.2	1.29		42.8	10.5
	47.1	1.29		42.0	9.4
	39.6	1.26		20.0	11.2
	27.3	1.22		18.0	10.2
	18.6	1.25			
	15.2	1.42	640	64.8	16.6
	7.15	1.90		48.0	18.3
				30.1	22.5
595	51.9	2.76		26.1	19.3
	51.5	2.70		19.7	19.7
	42.0	2.50		15.2	20.3
	41.7	2.80		13.7	20.8
	41.6	2.56			
	37.9	2.73			
	31.1	2.70			
	13.1	3.00			

In Table II a comparison is made of the velocity constants at 607° C. calculated from initial rates and those from t_{50}, t_{25}, and $t_{12.5}$. It will be seen that there is a steady fall in the value of the rate constant as we go from initial rates to $t_{12.5}$, t_{25}, and t_{50}. In other words the velocity constants fall off as a run proceeds, as is the case with all the paraffin hydrocarbons. The initial rates of reaction are, of course, the significant ones, and these only have been used in calculating the temperature coefficient, etc.

Over the relatively narrow range of pressure employed here, there is little definite evidence of a falling-off in rate with decreasing pressure. Actually, Sachsse found a considerable effect, but his measurements were made over a much wider range of pressure. Over the range from 10 to 50 cm., he observed only a slight effect, which is of the order of magnitude of the experimental error. It may therefore be concluded that his work is in agreement with ours on this point. In any case, the main object of the present investigation

TABLE II

COMPARISON OF RATE CONSTANTS AT 607° C.

Initial press., cm.	$K \times 10^4$, sec.$^{-1}$			
	From initial rates	From $t_{12.5}$	From t_{25}	From t_{50}
65.0	3.5	4.1	3.5	2.9
57.2	4.7	4.7	4.1	3.2
39.0	4.2	4.4	4.0	3.0
31.1	4.5	4.7	4.0	3.3
30.6	4.4	4.3	4.0	3.2
30.3	4.7	4.6	4.0	—
20.9	5.9	—	4.4	3.1
12.2	5.1	4.9	4.2	—
Mean	4.62	4.53	4.04	3.10

was the determination of the activation energy of the reaction. For this purpose only the higher pressure runs were employed. In Table III the mean values of the velocity constants from all high pressure runs are summarized.

TABLE III

MEAN VALUES OF RATE CONSTANTS FOR HIGH PRESSURE RUNS FROM INITIAL RATES

Temp., °C.	K, sec.$^{-1}$	Temp., °C.	K, sec.$^{-1}$
565	6.79×10^{-5}	607	4.62×10^{-4}
572	8.85×10^{-5}	616	7.43×10^{-4}
580	1.16×10^{-4}	625	1.05×10^{-3}
595	2.76×10^{-4}	640	1.71×10^{-3}

The values in Table III are shown in Fig. 1 in the form of a $\log_{10} K - 1/T$ plot. From the slope of the line we obtain for the activation energy the value 69.7 Kcal. Whence for the rate constant we have the expression

$$\log_{10} K = 14.02 - \frac{69700}{2.3RT} \text{ sec.}^{-1}$$

Activation energies were also calculated from the rate constants taken from $t_{12.5}$, t_{25}, and t_{50}. All these give values of the activation energy which are equal to the above value to within the experimental error.

The Products of the Reaction

A large number of analyses were made. In these a small quantity of methane was found, the quantity varying from 2 to 5% of that of ethylene. Since equilibrium corresponds only to 10 to 20% dissociation, in analyses at t_{50} there will be only 5 to 10% of ethylene present, and since the methane is only 2 to 5% of this, accurate analyses for methane were impossible. The quantity of higher hydrocarbons was also very small. The main products

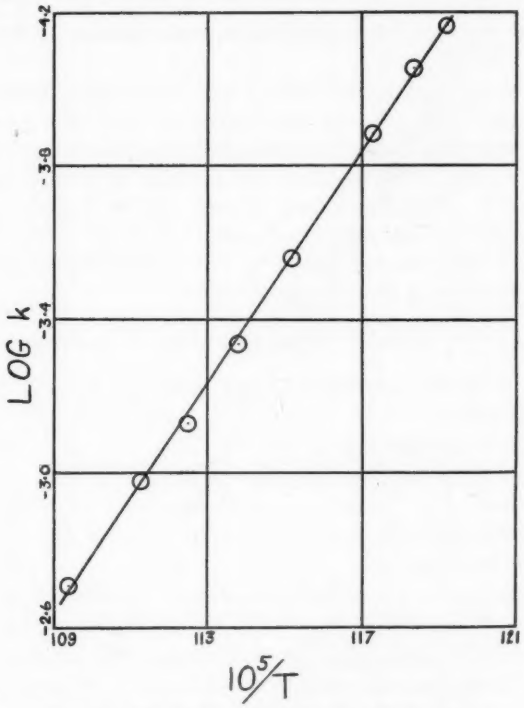

FIG. 1. *The temperature coefficient of the reaction.*

TABLE IV

THE PRODUCTS OF THE REACTION

Temp., °C.	Per cent decomposition $\left(\text{i.e., } \frac{x}{e} \times 100\right)$, calculated from pressure increase	Initial press., cm.	Moles C_2H_4 per mole H_2	Ratio of pressure increase calculated from H_2 and C_2H_4 formed to that observed
595	75.0	41.7	1.14	0.93
595	50.0	51.9	1.00	0.96
595	50.0	40.9	0.89	1.13
595	50.0	31.1	0.93	1.06
595	50.0	25.9	1.18	0.96
595	50.0	11.5	1.00	0.95
595	25.0	40.7	0.95	1.28
595	25.0	28.0	1.18	1.24
595	25.0	20.7	1.15	0.99
595	25.0	12.9	1.00	1.25
625	50.0	57.4	1.09	1.13
625	50.0	54.3	0.97	1.16
625	50.0	41.9	1.10	1.15
625	50.0	29.7	0.99	1.15
625	50.0	23.4	0.85	1.02
			Mean 1.02	1.09

of the reaction were, of course, hydrogen and ethylene. Analyses for these are given in Table IV.

It will be seen that within the rather large experimental error, the hydrogen and ethylene are equal. There are indications that the pressure increase observed is a little less than that calculated from the quantity of hydrogen and ethylene formed. This suggests the presence of a small amount of condensable products. Actually, traces of high boiling liquids were observed. The amount, however, was very small, and there is no doubt that the interpretation of the experimental results is not complicated to any appreciable extent by the presence of condensable products.

Discussion

A comparison of the activation energy found here with values of other workers is given below:

Marek and McCluer	73.2 Kcal.
Marek and McCluer (recalc.)	77.7
Sachsse	69.8
Küchler and Theile	77
This investigation	69.7

The main result of the present investigation is therefore to support strongly the lower values of the activation energy, especially that of Sachsse.

It should be emphasized that all investigations of the ethane decomposition are relatively inaccurate, on account of the difficulties associated with the back reaction. In an attempt to assess the situation, we have tabulated (Table V) the mean values of the velocity constants obtained by all workers.

These values are also given in Fig. 2 in the form of a log $K - 1/T$ plot. It will be seen from the figure that the results of Marek and McCluer are

TABLE V

SUMMARY OF RESULTS OF DIFFERENT OBSERVERS

Temp., °K.	Observer	Mean value of rate constant, sec.$^{-1}$	Temp., °K.	Observer	Mean value of rate constant, sec.$^{-1}$
824	Küchler and Theile	0.28×10^{-4}	889	This investigation	7.43
838	Storch and Kassel	0.60	898	Marek and McCluer	21.0
838	This investigation	0.68	898	This investigation	10.5
845	This investigation	0.89	910	Sachsse	20.8
853	This investigation	1.16	913	This investigation	17.1
856	Sachsse	1.83	922	Marek and McCluer	66.4
856	Küchler and Theile	1.5	934	Küchler and Theile	73
868	This investigation	2.76	938	Küchler and Theile	75
873	Marek and McCluer	7.9	941	Marek and McClure	136
880	This investigation	4.62	948	Marek and McCluer	294
886	Sachsse	7.4	973	Marek and McCluer	361
887	Küchler and Theile	7.8			

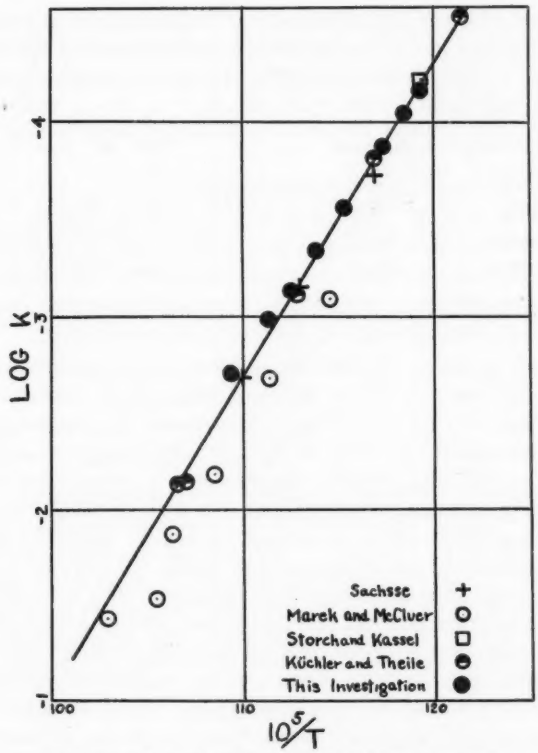

FIG. 2. *Comparison of results of different observers.*

definitely out of line with those of other workers. A "best" line through all the points also favours the lower estimates of the activation energy. This, however, is not very conclusive, since we would naturally expect that each worker's results would possess greater relative accuracy than absolute accuracy. However, all in all, the results to date favour an activation energy much below the value of 77 Kcal. given by Küchler and Theile, and it seems very unlikely that the true value of the activation energy is greater than 72 Kcal.

The absolute rates of reaction as determined by various observers are in much better agreement, especially in the low temperature range, than are the activation energies; thus for the velocity constant at 575° C., we have:

Marek and McCluer	1.7×10^{-4} sec.$^{-1}$
Marek and McCluer (recalc.)	1.0×10^{-4}
Sachsse	1.2×10^{-4}
Küchler and Theile	1.05×10^{-4}
Storch and Kassel	1.0×10^{-4}
This investigation	1.07×10^{-4}

The lower value of the activation energy is also supported by a comparison of the activation energies of the decomposition reactions of the lower straight chain paraffins. Thus, with our value for the activation energy of the ethane decomposition, we have

Substance	*E, Kcal.*	*Observer*
Methane	79.4	Kassel (9)
Ethane	69.7	This investigation
Propane	63.3	Steacie and Puddington (37)
n-Butane	58.7	Steacie and Puddington (35)

This gives a much more regular gradation of values than would a higher value for the activation energy of the ethane decomposition.

The low value of the activation energy found here has considerable bearing on the question of the role of free radicals in the ethane decomposition. The strength of the C—C bond in ethane is probably in the neighbourhood of 80 Kcal. If the activation energy of the over-all decomposition of ethane were 80 Kcal. also, no difficulty would be encountered in postulating an initial split into radicals. In this case, if subsequent reactions of radicals were fast compared with the primary split, the activation energy would be accounted for without the necessity of assuming reaction chains. The order of the reaction would also be accounted for, since if the primary split into radicals were a first order reaction, the over-all reaction would also be first order. If, however, the activation energy of the over-all reaction is much lower than that of the primary split, then the process can only be accounted for on a free radical basis by the assumption of long reaction chains. The low value of the activation energy found here, therefore, means that the ethane decomposition must involve long chains if it is a free radical process. The application of free radical mechanisms is thus made much more difficult.

The mechanism recently proposed by Küchler and Theile is based upon a value of the activation energy of 77 Kcal. Rice and Herzfeld (17) have discussed this mechanism in detail. They conclude that the mechanism proposed by Küchler and Theile is in agreement with thermochemical data. However, this can only just be done with certain assumptions and with a value of the activation energy ≥ 77 Kcal. Furthermore, their treatment contains a number of approximations such as the assumption of equal C—C and C—H bond strengths in methane and ethane. These render the treatment rather vague, but it appears probable that any adjustment in the right direction would necessitate an experimental activation energy greater than 77 Kcal. It therefore appears that the lower value of the activation energy supported by this investigation renders doubtful the Küchler and Theile mechanism.

It may also be pointed out that the present investigation supports a value for the frequency factor much lower than that found by Küchler and Theile, viz., 14.0 instead of 15.7. It appears on this basis that the value for ethane is not unusually high.

It should again be emphasized that the disagreement between the results of various observers is due to the experimental difficulties involved. As a consequence, the results for ethane are certainly less reliable than those for many other reactions. In view of this, it is suggested that some caution should be observed in the application of detailed chain mechanisms to the reaction.

Finally, it is of interest to compare the falling-off of the velocity constants with diminishing pressure for the lower paraffins. If K_∞ is the limiting high pressure rate constant at a given temperature, and K is the rate constant at the same temperature and a given pressure, then very roughly we have:

Substance	*Observer*	*Approx. pressure at which* $K_\infty/K = 1.5$
Ethane	Sachsse	70 – 90 mm.
Propane	Steacie and Puddington	60 – 80 mm.
n-Butane	Steacie and Puddington	170 – 220 mm.
Isobutane	Steacie and Puddington	40 – 60 mm.

If the paraffin decompositions were ordinary first order reactions, we would expect the more complex molecules to show the falling-off at much lower pressures than the simpler ethane molecule. As a matter of fact, in the case of an homologous series such as the nitrite decompositions (28), the variation of falling-off pressure with molecular complexity is entirely regular. The complete lack of regularity here seems to be strong evidence that at least the higher members of the series must decompose by chain mechanisms.

References

1. Dintzes, A. I. and Frost, A. V. J. Gen. Chem. U.S.S.R. 3 : 747-758. 1933.
2. Dintzes, A. I. and Frost, A. V. Compt. rend. acad. sci. U.R.S.S. 4 : 153-157. 1934.
3. Dintzes, A. I. and Frost, A. V. Compt. rend. acad. sci. U.R.S.S. 5 : 513. 1934.
4. Dintzes, A. I., Zharkova, V. R., Zherko, A. V., and Frost, A. V. J. Gen. Chem. U.S.S.R. 7 : 1063-1070. 1937.
5. Echols, L. S. and Pease, R. N. J. Am. Chem. Soc. 58 : 1317. 1936.
6. Frey, F. E. and Smith, D. F. Ind. Eng. Chem. 20 : 948-951. 1928.
7. Gorin, E., Kauzmann, W., Walter, J., and Eyring, H. J. Chem. Phys. 7 : 633-644. 1939.
8. Hobbs, J. E. and Hinshelwood, C. N. Proc. Roy. Soc. London, A, 167 : 439-446. 1938.
9. Kassel, L. S. J. Am. Chem. Soc. 54 : 3949-3961. 1932.
10. Küchler, L. and Theile, H. Z. physik. Chem. B, 42 : 359-379. 1939.
11. Marek, L. F. and McCluer, W. B. Ind. Eng. Chem. 23 : 878-881. 1931.
12. Patat, F. and Sachsse, H. Z. Elektrochem. 41 : 493-494. 1935.
13. Pease, R. N. J. Am. Chem. Soc. 50 : 1779-1785. 1928.
14. Paul, R. E. and Marek, L. F. Ind. Eng. Chem. 26 : 454-457. 1934.
15. Rice, F. O. and Herzfeld, K. F. J. Am. Chem. Soc. 56 : 284-289. 1934.
16. Rice, F. O. and Teller, E. J. Chem. Phys. 6 : 489-496. 1938.
17. Rice, F. O. and Herzfeld, K. F. J. Chem. Phys. 7 : 671-673. 1939.
18. Sachsse, H. Z. physik. Chem. B, 31 : 79-86. 1935.
19. Sachsse, H. Z. physik. Chem. B, 31 : 87-104. 1935.
20. Sickman, D. V. and Rice, O. K. J. Chem. Phys. 4 : 608-613. 1936.
21. Staveley, L. A. K. Proc. Roy. Soc. London, A, 162 : 557-568. 1937.
22. Steacie, E. W. R. J. Chem. Phys. 6 : 37-40. 1938.

23. STEACIE, E. W. R. Chem. Rev. 22 : 311-402. 1938.
24. STEACIE, E. W. R., ALEXANDER, W. A., and PHILLIPS, N. W. F. Can. J. Research, B, 16 : 314-318. 1938.
25. STEACIE, E. W. R. and BROWN, E. A. Unpublished work.
26. STEACIE, E. W. R. and FOLKINS, H. O. Can. J. Research, B, 17 : 105-120. 1939.
27. STEACIE, E. W. R. and FOLKINS, H. O. Can. J. Research, B, 18 : 1-11. 1940.
28. STEACIE, E. W. R. and KATZ, S. J. Chem. Phys. 5 : 125-130. 1937.
29. STEACIE, E. W. R. and PARLEE, N. A. D. Trans. Faraday Soc. 35 : 854-860. 1939.
30. STEACIE, E. W. R. and PARLEE, N. A. D. Can. J. Research, B, 17 : 371-384. 1939.
31. STEACIE, E. W. R. and PHILLIPS, N. W. F. J. Chem. Phys. 4 : 461-468. 1936.
32. STEACIE, E. W. R. and PHILLIPS, N. W. F. J. Chem. Phys. 5 : 275. 1937.
33. STEACIE, E. W. R. and PHILLIPS, N. W. F. J. Chem. Phys. 6 : 179-187. 1938.
34. STEACIE, E. W. R. and PHILLIPS, N. W. F. Can. J. Research, B, 16 : 303-313. 1938.
35. STEACIE, E. W. R. and PUDDINGTON, I. E. Can. J. Research, B, 16 : 176-193. 1938.
36. STEACIE, E. W. R. and PUDDINGTON, I. E. Can. J. Research, B, 16 : 260-272. 1938.
37. STEACIE, E. W. R. and PUDDINGTON, I. E. Can. J. Research, B, 16 : 411-419. 1938.
38. STORCH, H. H. and KASSEL, L. S. J. Am. Chem. Soc. 59 : 1240-1246. 1937.
39. TAYLOR, H. S. J. Phys. Chem. 42 : 763-772. 1938.
40. TRAVERS, M. W. J. Indian Chem. Soc. P.C. Ray Commemoration Volume, pp. 17-26. 1933.
41. TRAVERS, M. W. Trans. Faraday Soc. 33 : 735-751. 1937.
42. TRAVERS, M. W. and HOCKIN, L. E. Proc. Roy. Soc. London, A, 136 : 1-27. 1932.
43. TRAVERS, M. W. and PEARCE, T. J. P. J. Soc. Chem. Ind. 53 : 321T-336T. 1934.
44. TRENNER, N. R., MORIKAWA, K., and TAYLOR, H. S. J. Chem. Phys. 5 : 203-211. 1937.

THE CONSTRUCTION AND OPERATION OF A SIMPLE AUTOMATIC MULTIPLE BURETTE[1]

By J. S. Tapp[2]

Abstract

A simple automatic machine has been designed and built for delivering small measured quantities of liquid at regular intervals of time. The fluid comes in contact with no other material than glass, and hence the apparatus may be used to handle almost all known, free flowing liquids without fear of corrosion of the apparatus or serious contamination of the fluid. The liquid may contain a solute or stable colloidal particles without causing irregular operation through the deposition of solids by evaporation. The design lends itself particularly to handling many different fluids simultaneously, or to delivering measured quantities of a similar fluid at many different places.

A machine substantially similar to the one described in this paper, handling 12 different fluids at once, has been in operation continuously for more than eight months, and has required very little attention apart from replenishing the contents of the reservoirs.

Details of Construction

The apparatus consists essentially of a number of burette-reservoir units, similar to that shown in Fig. 1, and of one control unit connected with and operating the battery of burette-reservoir units. The maximum number of units which may be operated by one control is unknown; 12 have worked satisfactorily, and, with no modification of the valves, it appears certain that three to four times that many could be handled equally well.

The construction of the burette and reservoir is not complicated, nor does its successful operation depend upon adherence to strict dimensional accuracy. With reference to Fig. 1, the burette was made from the upper portion of an ordinary Pyrex test tube which had been drawn down to about $\frac{1}{4}$ in. inside diameter at a point about 4 in. from its open end. The tube was cut at the constriction and a piece of Pyrex tubing about 1 in. long and $\frac{1}{4}$ in. inside diameter was sealed on and closed at its other end. The side arm ending at H_1 was drawn down from 1 cm. diameter Pyrex tubing so that it had an internal diameter of about 2 mm. The end was further reduced in size to a nozzle of about 1 mm. bore. Each unit was roughly similar in dimension at this point. Small differences were unimportant but no nozzle should be more than twice as large as the size decided upon in advance. The tube ending at H_3 and extending to near the bottom of the reservoir was 4 or 5 mm. internal diameter and tapered down at the end, H_3, so that its external diameter was not more than half nor less than one-third the inside diameter of the surrounding tube. The end was cut off straight across and lightly ground on fine emery cloth. The reservoir was a 250 cc. bottle fitted with a two-hole

[1] *Manuscript received February 28, 1940.*

Contribution from the Division of Chemistry, National Research Laboratories, Ottawa, Canada. Issued as N.R.C. No. 916.

[2] *Chemist.*

rubber stopper. The tubes L_1 and L_2 were attached in the position shown in the same diagram.

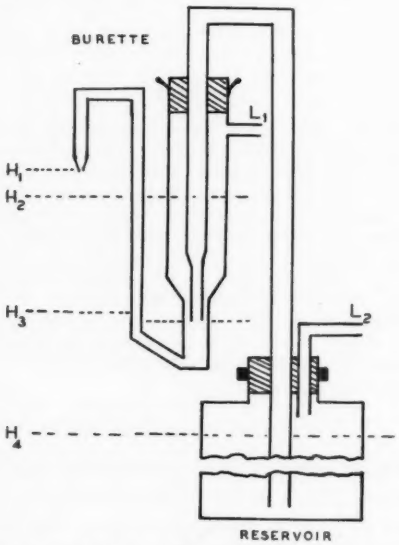

FIG. 1. *Diagram of a single burette-reservoir unit.*

The following constructional details in Fig. 1 are important:

(i) The highest level of fluid in the reservoir, say H_4, must be at least 1 in. below the level of H_3.

(ii) The level H_1 must be not less than 3 in. above H_3.

(iii) The tube L_1 must be at least $\frac{1}{2}$ in. above H_2.

(iv) The volume contained below H_3 in the burette is the volume of fluid dispensed at each cycle of operation; obviously, this can be adjusted as desired between limits governed by the over-all dimensions. In the apparatus which is in operation in this laboratory, this volume is 0.6 cc. It could be increased to about 1 cc. or decreased to about 0.1 cc. by merely adjusting the position of H_3 above the bottom of the burette.

The control unit was made up of five cams A to E, Fig. 2, on a common shaft. Cams A to D operated valves A_1 to D_1, respectively, through rocker arms pivoted on a common shaft. The valves were short pieces of light rubber tubing, which were pinched against a wooden block by the rocker arms. The arms were caused to follow the cams by springs conveniently mounted but not shown in the diagram. The cams were made from pieces of brass rod $\frac{3}{4}$ in. in diameter and each was fitted with a hub and setscrew for securing it to the shaft. The cam action was obtained by drilling and tapping the rim of each disc for a small machine screw, which could then be screwed in or out as desired to vary the amount of lift. Each screw had a lock nut, not shown

in the diagram. Cam *A* had two such lifts separated by an angle of 130° and cam *C* was recessed over an angle of 90°.

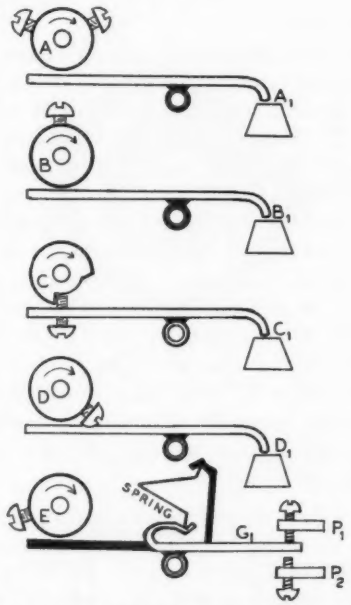

FIG. 2. *Diagram of the five cams and rocker arms which made up the control unit.*

Cam *E* operated part of the electrical control for the motor which rotated the camshaft through suitable gearing. The other part of the electrical control was located elsewhere and was operated by cam *F*, Fig. 3, which in turn was driven through gearing by an electric motor that ran continuously. This motor could very readily be a synchronous one, in which case the timing would be quite accurate. It was found, however, that an ordinary $\frac{1}{8}$ h.p., a-c. motor driving a moderate but continuous load, aside from cam *F*, gave sufficiently accurate time intervals. The interval used was 20 min.; i.e., cam *F* turned once every 20 min., which could be altered to a minimum of 2 min. or to a maximum limited only by the multiplicity of the gear train employed. Essentially, the speed of cam *F* governed the length of time between operations

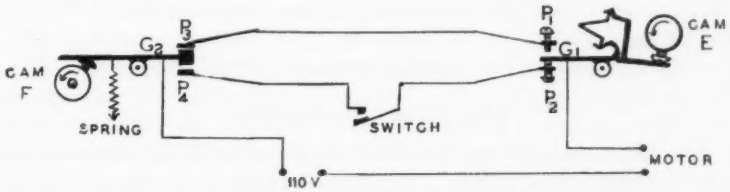

FIG. 3. *Diagram of the electrical connections.*

of the burette, while cam E served only to stop the rotation of the valve cams when a single cycle of operation had been completed. Cams F and E may be separated by any convenient distance since they are connected only through three insulated wires.

The stationary electrical contacts P_1, P_2, P_3, and P_4 were simple brass contacts. The contact G_2 was insulated from the pivot, spring, and cam, but was mechanically continuous throughout. The other contact G_1 is most clearly shown in Fig. 2. The arm operated by the cam E pivoted freely on the common rocker-arm shaft and extended upwards beyond the pivot as shown by the shaded portion of the drawing. The unshaded portion of the arm, indicated by G_1, also pivoted around the same point, but was mechanically connected to the rocker arm only through the medium of the V-shaped spring, shown most clearly in Fig. 2. This spring pressed outwards and was restrained only at the two extremities. The result of this construction was that contact G_1 was always touching *either* P_1 or P_2 except for the small interval of time during which it snapped from P_1 to P_2 or the reverse. Since the camshaft, and hence cam E, turns quite slowly (one revolution in about 30 sec.), and stops almost instantly whenever G_1 breaks contact with either P_1 or P_2, it is essential for G_1 to be touching one or other of the contacts and not stopped somewhere between.

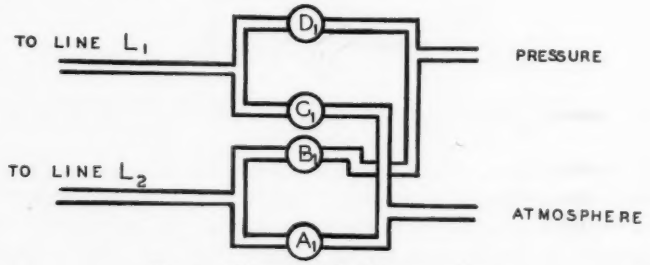

FIG. 4. *Diagram of the valve connections.*

Fig. 4 shows the way in which the valves were connected between the air pressure and the lines L_1 and L_2. The tube marked "atmosphere" served as a pressure release; the tube marked "pressure" was kept at about 7 lb. gauge air pressure from the 80 lb. line through a suitable reducing valve. The lines L_1 and L_2 in Fig. 4 were copper tubes $\frac{1}{8}$ in. inside diameter, with one side tube soldered on each line for each burette-reservoir unit under control. Short lengths of rubber tubing connected one side tube from each line to the openings marked L_1 and L_2 in Fig. 1. If lines L_1 and L_2 in Fig. 4 are over 6 ft. long, the copper tubing should be $\frac{1}{4}$ in. inside diameter to insure reliable operation.

The Cycle of Operation

Fig. 5 is a diagrammatic representation of the valve timing where the shaded portions represent *closed* valves. The outer annulus gives the position of the electrical switch G_1, i.e., whether in contact with P_1 or P_2. With reference

to all five diagrams, the following sequence of operation takes place automatically and at intervals of time depending on the speed of cam *F*.*

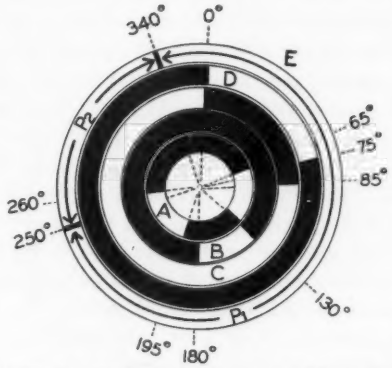

FIG. 5. *Timing diagram of the five cams of the control unit.*

Cam *F*, Fig. 3, turns slowly but continuously and the contact G_2 is caused to touch the point P_4. (The manual control switch in Fig. 3 has been closed by hand.) This completes the circuit through G_2, P_4, P_2, G_1, and the cams *A* to *E* begin to revolve. Still with reference to Fig. 3, cam *E* soon allows its rocker arm to rise and contact G_1 snaps up from P_2 to P_1 breaking the electrical circuit established a few moments before; cams *A* to *E* stop about 15° counterclockwise from the position shown in Fig. 2, and the cycle is in the position represented by the 340° mark in Fig. 5.

Cam *F*, Fig. 3, continues to turn and finally allows the contact G_2 to be pulled up by the spring to P_3. When this happens, the electrical circuit G_2, P_3, P_1, G_1 is completed and the cycle proper begins. At the arbitrary 0° mark in Fig. 5 or in the exact position of the cams as shown in Fig. 2, valve C_1 closes and valve D_1 begins to open, and pressure enters the line L_1 (see Fig. 4). The liquid in the burette is forced up the side arm and out the nozzle H_1, and is at that point available for any desired purpose in the prescribed quantity. The valve D_1 remains open for 75° of camshaft rotation and during that time air under pressure is entering L_1 of the burette. At 65°, valve A_1 begins to open; this connects line L_2 to the atmosphere, thereby releasing any air which has bubbled over into the reservoir. At 85°, valve C_1 begins to open and at once releases any residual air pressure in the line L_1 after D_1 has closed. The precision of this particular sequence is most important for the successful operation of the machine. At 130°, A_1 closes and B_1 opens; this admits pressure to line L_2 and forces some of the liquid in the reservoir up through the long tube into the burette. Valve B_1 remains open to 180° and then valve A_1 opens again at 195°. The flow of liquid to the burette continues until valve A_1 opens and releases the pressure in the line L_2. The

* *In Fig. 1 the burette will have been filled with liquid to the level of H_3 through the operation of the previous cycle.*

amount of liquid delivered to each one of the numerous burette units during this period of operation is not the same for each unit, since the quantity depends almost entirely upon the dimension of the nozzle at H_3. However, the amount must lie somewhere between the volumes represented by the levels H_3 and H_2. This gives ample tolerance for easy construction.

At 195°, valve A_1 opens, and, since C_1 is also open, both lines L_1 and L_2 are at atmospheric pressure, and the liquid in the burette above the level of H_3 begins to syphon back into the reservoir. Before this has been completed, the electrical contact G_1, at 250°, has snapped from P_1 to P_2, thus interrupting the circuit G_2, P_3, P_1, G_1, and as a result the cams A to E have stopped. Valves A_1 and C_1 remain open and the liquid continues to syphon back into the reservoir until the syphon is broken by the level coming to H_3. This leaves a definite quantity of liquid in the burette which is in no way altered by the level to which the liquid has risen in the burette prior to the beginning of syphoning. It is with this definite quantity of liquid in the burette that the cycle just described began.

Cam F, Fig. 3, continues to turn and finally connects G_2, P_4, P_2, G_1, and the cams A to E again begin to revolve. Valve A_1 closes at 260°; this is unimportant as long as it closes before 0° is reached. At 340°, contact G_1 P_2 changes to G_1 P_1 and the cams A to E stop again. Once more, cam F permits the G_2, P_3, P_1, G_1 circuit to be completed, and the major cycle begins at 340° with the valves beginning to operate at the 0° mark.

Each time that the arbitrary reference point on the cam shaft passed 85° in the timing cycle a Veeder counter was tripped; this recorded the delivery of the prescribed amount of fluid. Daily or weekly recording of the figures on the Veeder kept the operator posted on the quantity of fluid delivered over an interval of time.

CANADIAN JOURNAL OF RESEARCH

Notes on the Preparation of Copy

General:—Manuscripts should be typewritten, double spaced, and the original and one copy submitted. Style, arrangement, spelling, and abbreviations should conform to the usage of this Journal. Names of all simple compounds, rather than their formulae, should be used in the text. Greek letters or unusual signs should be written plainly or explained by marginal notes. Superscripts and subscripts must be legible and carefully placed. Manuscripts should be carefully checked before being submitted, to reduce the need for changes after the type has been set. All pages should be numbered.

Abstract:—An abstract of not more than about 200 words, indicating the scope of the work and the principal findings, is required.

Illustrations:—Drawings should be carefully made with India ink on white drawing paper, blue tracing linen, or co-ordinate paper ruled in blue only. Paper ruled in green, yellow, or red should not be used. The principal co-ordinate lines should be ruled in India ink and all lines should be of sufficient thickness to reproduce well. Lettering and numerals should be of such size that they will not be less than one millimetre in height when reproduced in a cut three inches wide. If means for neat lettering are not available, lettering should be indicated in pencil only. All experimental points should be carefully drawn with instruments.

Illustrations need not be more than two or three times the size of the desired reproduction, but the ratio of height to width should conform with that of the type page. Small photographs should be mounted on cardboard and those to be reproduced in groups should be so arranged and mounted. The author's name, title of paper, and figure number should be written on the back of each illustration. Captions should not be written on the illustrations, but typed on a separate page of the manuscript.

Tables:—Titles should be given for all tables, which should be numbered in Roman numerals. Column heads should be brief and textual matter in tables confined to a minimum.

References should be listed alphabetically by authors' names, numbered in that order, and placed at the end of the paper. The form of literature citation should be that used in this Journal and titles of papers should not be given. All citations should be checked with the original articles.

The *Canadian Journal of Research* conforms in general with the practice outlined in the *Canadian Government Editorial Style Manual*, published by the Department of Public Printing and Stationery, Ottawa.